

The Mineralogical and Chemical Composition of the Strongly Magnetic Egyptian Black Sand Altered Ilmenite

Mohamed Ismail Moustafa

Nuclear Materials Authority, Egypt

ismail2251962@yahoo.com

Received: 9 May 2023 | Revised: 30 May 2023 | Accepted: 6 June 2023

Licensed under a CC-BY 4.0 license | Copyright (c) by the authors | DOI: <https://doi.org/10.48084/etasr.6025>

ABSTRACT

The Egyptian black sand contains several types of altered ilmenite grains which have various magnetic susceptibility values, ranging from the strongly paramagnetic, such as ilmenite, to the non-magnetic, such as rutile grains. The altered ilmenite grains of relatively higher mass magnetic susceptibility, separated at 0.1, 0.2, 0.25, and 0.35 A using the Frantz isodynamic magnetic separator, were investigated. Both brown and black altered grains were investigated using the binocular microscope and the Cameca SX-100 microprobe. Most analyzed spots of grains are composed mainly of pseudorutile (psr) and leached pseudorutile (lpsr), with the contents of TiO₂ and Fe₂O₃ ranging between 56.76 and 78.09% and 37.98 and 12.16%, respectively. The Ti/(Ti+Fe) ratio ranges between 0.59 and 0.85. The chemical formula range of the investigated psr-lpsr is Fe_{2.07-0.54}Ti₃O_{9-4.68}(OH)_{0-4.32}. The lowest cationic iron content of the lpsr phase is 0.5 with a corresponding molecular formula of Fe_{0.5}Ti₃O_{4.5}(OH)_{4.5}. In the detected leached ilmenite spots, the cationic Fe²⁺ ranges between 0 and 2.46, while the cationic Fe³⁺ ranges between 0.17 and 1.94. The Ti/(Ti+Fe) ratio ranges between 0.51 and 0.6, and the Fe/Ti ratio ranges between 0.91 and 0.67. Considering the chemical formula of ilmenite is Fe₂Ti₃O₉, the leached ilmenite formulas have the composition Fe_{2.72-2.02}Ti₃O₉ with the minimum value of total iron being equal to 2.02. Some of the contained inclusions may be responsible for the acquired magnetic characteristics of some of the detected altered grains. The powdered X-ray diffraction patterns of the investigated different magnetic grains were detected before and after heating at 1100 °C for one hour. The hexagonal psr/lpsr structure is more unstable at 1100 °C than the tetragonal rutile structure. According to the calculations of the molecular formulas for the detected alteration phases, the lowest iron content of the altered lpsr is much lower than that previously reported. Also, during the alteration process, the alteration mechanism is changed in the region of 68-70 wt % of contained TiO₂. Then, in the late alteration stages, the lpsr structure does not suddenly collapse but gradually produces other associated mineral phases.

Keywords-Egypt; black sand; magnetic; nonmagnetic; leucoxene; leached ilmenite; leached pseudorutile

I. INTRODUCTION

The discovery of a new mineral, arizonite, of a chemical composition closely corresponding to Fe₂O_{3.3}TiO₂ was reported in [1]. Arizonite is regarded as merely weathered ilmenite [2]. According to [3], most of the studied ilmenite concentrates from several beach sand deposits contain ore grains ranging from fresh ilmenite to a highly altered product approaching pure TiO₂ in composition. The nature and chemical composition of leucoxene are known to be variable [4]. Leucoxene is commonly considered to be microcrystalline rutile [3, 5-7]. Occasionally some leucoxene have also yielded X-ray patterns corresponding to either sphene [4], brookite [4, 5, 7], anatase [5], or mixtures of rutile with anatase or brookite [7]. There is an abundance of co-occurrence of pseudobrookite and altered ilmenite in Quilon sands, India [8]. However, the authors in [9] do not agree with Karkhanavala's explanation unless the primary pseudobrookite was early present in the source area. When the ilmenite structure is broken down by

alteration and the material is turned amorphous, a marked decrease in mass magnetic susceptibility, an increase in TiO₂ and H₂O contents and a high Fe³⁺/Fe²⁺ ratio occur. The term hydroilmenite is given for the obtained amorphous phase [10]. In fact, authors in [11] prefer the term altered or weathered ilmenite since the chemical and mineralogical composition varies with the degree of alteration, and the amount of water present is very small.

The name pseudorutile is proposed for the product of oxidation and progressive partial removal of iron due to the alteration of ilmenite giving an intermediate iron titanate of a definite structure [12]. The identification of the intermediate altered compound pseudorutile was difficult in earlier studies due to its occurrence in fine grain size (30 °A), its poor crystallinity, and its coincidence for most of its diffraction lines with those of other phases [13]. Thus, it is safe to say that the distinct isotropic phase, previously called arizonite [1],

amorphous iron titanate [6], and pro-arizonite [14], is pseudorutile.

Many grains of ilmenite may remain unchanged for long burial times, perhaps at shallow depth, but below the oxidation zone [15]. Authors in [15] believe that the major part of the alteration of the sand ilmenite takes place neither in the crystalline rocks nor on the beach, but while they were buried in sediments during their journey. Authors in [16, 17] agree that ilmenite may be altered under reducing conditions. On the other hand, authors in [18] explained that the rate of alteration of ilmenite to secondary TiO_2 might control the formation of a polymorph. Also, the occurrence of impurities affects the formation of polymorphic forms. According to [19], the change from ilmenite to psr involves a phase change in the oxide structure. Aluminum and silicon are also enriched due to the iron depletion during the first stage of alteration, but their concentrations remain quite low, i.e. $Al_2O_3 \leq 0.4$ wt % and $SiO_2 \leq 0.1$ wt % [20]. For $Ti/(Ti+Fe) > 0.7$, corresponding to the second stage of alteration proposed by [21], the aluminum and silicon levels increase rapidly with increasing $Ti/(Ti+Fe)$ ratios, to maximum values near 1.5 wt % Al_2O_3 and 0.5 wt % SiO_2 . This increase is due to the co-precipitation or adsorption of these elements from the surrounding soil solutions onto the freshly-formed alteration products.

The occurrence of gibbsite and clay minerals within the pores of the weathered grains was reported in [22]. The authors explained the increase of Al and Si contents with the increase of $Ti/(Ti+Fe)$ ratio as a consequence of the increase of the abundance of pores available for the crystallization of clay minerals, as ilmenite and pseudorutile alter isovolumetrically to porous rutile. According to [23], the model of [21] has several weaknesses, the two model's reactions require different environments to proceed, the first an oxidizing one and the second a reducing one with its reliance on reducing conditions in near surface conditions. Authors in [24] explained that the detrital ilmenite grains of heavy mineral sands in Brazil are extremely altered sometimes in psr and anatase (grain boundaries), and also leucoxene. In some leucoxenated grains of the Egyptian black sand, residual particles of ilmenite are enclosed in many of the altered ilmenite grains and a few grains still preserved the crystal form of the parent ilmenite [25]. The mineralogy of the Egyptian black sand ilmenite is well defined in [26, 27]. In [28], most of the given individual examples of psr and lpsr are considered ideal cases with respect to their given values of TiO_2 and FeO, the reverse relation between these two oxides, and the values of the total oxide sum. The given examples of the three analyzed psr spots were: the TiO_2 wt % contents were 62.16, 64.62, and 66.04, respectively, the FeO wt % contents were 28.28, 25.62, and 24.21, respectively, and the total oxide sum values were 93.71, 92.98, and 92.67, respectively. Also, the given examples of the lpsr spot chemical analysis were: the TiO_2 wt % contents were 70.67, 72.02, and 74.57, respectively, the FeO wt % contents were 15.79, 13.95, and 10.32, respectively, and the total oxide sum values were 89.96, 88.18, and 89.08, respectively.

It is obvious from the above, that most literature dealt with bulk ilmenite concentrates from friable sediments (e.g. beach sand deposits). A few studies dealt with the altered ilmenite

from sedimentary and igneous rocks. Most depended in their investigation on the microscopic investigation, microprobe chemical analysis, and the XRD identification. Also, almost all past studies dealt with the occurrence of Al_2O_3 and SiO_2 contents in the altered ilmenite phases considering both as impurities. In the present study, some of the strongly magnetic altered ilmenite grains are investigated to explain their mineralogical and chemical composition characters. The purpose of the current work is to detect the different lpsr phases, the lowest iron content in these phases, and the most stable molecular formulas of the detected lpsr phases. Also, the real role of SiO_2 and Al_2O_3 contents in ilmenite alteration will be checked. Several Excel sheets were constructed to solve the chemical formulas of the various ilmenite alteration products.

II. MATERIALS AND METHODS

A large bulk sample was collected from the surficial naturally highly concentrated black sand from the beach area at the Mediterranean coast, 7 km to the east of Rosetta estuary, Egypt. The sample represents the raw sand in a 4 km stretch with a variable width of a few up to 20 meters. The sand was manually scraped from the mantle to a depth ranging between 10 and 30 cm. Using the difference in physical character between the various minerals, the collected surficial naturally highly concentrated beach raw sand was processed using the following equipment:

1. The reading cross-belt magnetic separator for primary magnetic separation.
2. Full size Wilfley shaking tables for wet-gravity concentration of the obtained bulk nonmagnetic fraction.
3. The Carpco (HP 167) high-tension roll-type electrostatic separator for treating the obtained tabled concentrate of the last obtained nonmagnetic fraction.
4. The Carpco (MIH 13-231-100) industrial high intensity induced roll dry magnetic separator for the magnetic separation of the obtained rutile conductor fraction.
5. The Frantz isodynamic magnetic separator. The last obtained three successive magnetic fractions were mixed as a bulk magnetic fraction, composed of hematite, ilmeno-hematite, different varieties of magnetic primary rutile [29], and various grades of altered ilmenite grains, in addition to minor Cr-bearing and other magnetic minerals [30]. A relatively smaller representative sample was obtained from the bulk magnetic fraction and was subjected to magnetic differentiation using the separator where the used adjustments of operating conditions were: longitudinal slope of 20° , side slope of 5° , feeding rate of 30 g/hour, and successive current values of 0.1, 0.2, 0.25, 0.35, 0.5, and 1 A, where six magnetic fractions and one nonmagnetic fraction were obtained. In the present paper, only the first four magnetic fractions, separated at 0.1, 0.2, 0.25 and 0.35 A are investigated.
6. The microprobe analysis. The investigation of the different altered ilmenite grains was carried out by a Cameca SX-100 Electron Micro Probe analyzer (EMPA). The

microprobe instrument is equipped with three Wavelength Dispersive Spectrometers (WDSs) and an Energy Dispersive Spectrometer (EDS). The whole surface of the polished sections was examined by Back Scattered Electron (BSE) images, so that grains with 10 μm size, or even smaller, could be detected. The conditions were: 15 kV accelerating voltage, 15 nA electron current, 180 s counting time for each analyzed spot in the investigated grains, and a focused electron beam diameter of 1 to 4 μm . The following standards were used: diopside for Mg and Ca, albite for Na, corundum for Al, orthoclase for Si and K, rutile for Ti, rhodonite for Mn, Fe_2O_3 for Fe, Cr_2O_3 for Cr, V for V, and sphalerite for Zn. The lines used for the analysis were $K\alpha$ for each of the analyzed elements. For each detected altered ilmenite variety, a definite number of grains was picked individually and polished for the investigation using the microprobe.

- The X-Ray Diffraction (XRD) instrument. Philips X-ray generator (PW 3710/31) with automatic sample changer (PW 1775, 21 positions) using a scintillation counter, Cu-target tube and Ni filter at 40 kV and 30 mA were used. This instrument is connected with a computer system using the X-40 diffraction program and ASTM cards for mineral identification.

III. CALCULATIONS

The calculations of trivalent iron, H_2O , and the chemical formulas for the intermediate products of ilmenite alteration were carried out after the calculation of the following two values [28]:

- The molecular proportion for each analyzed oxide was obtained by dividing its analyzed wt % by its molecular weight. For all altered phases, the analyzed iron is given as FeO wt %.
- The mole % for each cation on the basis of $\text{Ti}=3$, considering that the ilmenite formula is $[\text{3}(\text{FeTiO}_3)]$. An example is the calculation of the mole % of Si, which is equal to $3 \times [\text{SiO}_2 \text{ (mole proportion)}/\text{TiO}_2 \text{ (mole proportion)}]$.

The authors in [28] do not give any explanation about the various used steps in their calculations. They gave three individual examples of the calculation results for each of leached ilmenite, pseudorutile, and leached pseudorutile phases. In these 9 examples, they considered the mole % for each cation as the same as the mole % value of its corresponding oxide irrespective of the number of cations in the oxides molecular formula. In fact, the chemical analyses of various ilmenite ores do not contain only FeO, MgO, MnO, CaO, TiO_2 , SiO_2 , and ZnO but may contain relatively higher contents of V_2O_3 , Cr_2O_3 , Nb_2O_3 , Ta_2O_3 , Fe_2O_3 , and/or Al_2O_3 and maybe others. So, it is better to take the number of cations in the corresponding oxide into consideration in the calculation of the cation mole %. Also, in the calculation of ferric iron (Fe^{3+}) in the cases of pseudorutile and leached pseudorutile chemical formulas, the authors in [28] considered that the mole % of Fe^{3+} is equal to that of the divalent iron Fe^{2+} in the

analyzed FeO% multiplied by 1.1113. However, this factor is related to the difference of the oxygen content between the oxides FeO and Fe_2O_3 . In fact, the cationic ferrous iron content of the analyzed iron as FeO must be the same as that of the corresponding Fe_2O_3 when FeO is recalculated as Fe_2O_3 . In one of the given three examples of psr, the mole% of FeO and hence of Fe^{2+} is calculated as 1.223 and the recalculated mole% of Fe^{3+} is 1.36, which is 1.223×1.1113 . This method of calculation was followed for all the given six examples, three for psr and three for lpsr, see Tables 2-3 in [28]. However, a relatively more precise method for the calculation of Fe^{3+} content from the analyzed FeO wt % in ilmenite was given in [31]. The authors considered the value exceeding 1 for the calculated mole% of Fe^{2+} from the analyzed FeO, as corresponding to the present Fe^{3+} as $\text{FeO}_{1.5}$. Then by multiplying the excess, e.g. 0.12 as given from their example, in 1.1113 and by dividing the obtained value by 2, the mole % of Fe_2O_3 (0.067) is obtained.

The various constructed Excell spreadsheets in the present study are:

A. The Constructed Molecular Formula of Leached Ilmenite

In the construction of the molecular formula of leached ilmenite ($\text{Fe}^{2+}_3\text{Ti}_3\text{O}_9$), the iron content of the analyzed spots of leached ilmenite is given as FeO wt % and the number of cations in the analyzed cation oxide molecular formula is taken into consideration. The adopted procedure includes the following steps:

- The calculation of the molecular proportion for each analyzed oxide of each spot of an individual ilmenite grain.
- The calculation of Ti-factor which equals to 3 divided by the calculated molecular proportion of the analyzed TiO_2 wt % of each individual analyzed spot.
- The calculation of the number of cations of each analyzed oxide after the normalization to 3 Ti (mole % cations). Hence, the calculated molecular proportion of the oxide will be multiplied in the Ti-factor and also, in the number of cations present in its corresponding analyzed oxide formula.
- The calculation for the sum of all cation numbers except those of Ti and Fe. This sum is called "other cations".
- The calculation of the sum of all cation charge values (W1), except those of Ti and Fe, by summation of each cation mole % \times cation charge.
- Considering that $Y = \text{Fe}^{3+}$, $X = \text{Fe}^{2+}$, K is the content of the mole % of total iron (iron cations normalized to 3 Ti), then the sum of the quotients of the total anionic charges. $\text{O}9 = -18$ and total cation charges, $(3Y + 2X + W1 + 3\text{Ti}^{4+})$, must be equal to zero:

$$X + Y = K, \text{ then, } X = K - Y \quad (1)$$

Then:

$$3Y + 2X + W1 + 3\text{Ti}^{4+} - 18 = 0$$

Then:

$$3Y + 2(K - Y) + W1 + 12 - 18 = 0$$

$$\text{and } Y = 6 - (W1 + 2 K) \quad (2)$$

Because the number of cations in the calculated mole % of each cation will be taken into consideration, the value of the calculated cationic charges for the analyzed minor oxides containing cations that have oxidation states more than that of Fe^{2+} , such as Al^{3+} , Cr^{3+} , V^{3+} , Nb^{5+} , and Ta^{5+} , will considerably affect the calculated values of X and Y. However, their summation (X+Y) is always equal to K.

- The calculation of the new FeO wt % equals to:

$$\text{The original analyzed FeO wt \%} * X/(X+Y) \quad (3)$$

- The calculation of the contained Fe_2O_3 wt % equals to:

$$\text{The original analyzed FeO wt \%} * Y/(X+Y) \quad (4)$$

- The determination of the molecular formula will be:

Fe^{2+} Ferrous, Fe^{3+} Ferric, other cations, Ti_3 , O_9 .

B. The Constructed Molecular Formula of Pseudorutile and Leached Pseudorutile

1) The First Method of Calculating the Number of Oxygen Anions and the Number of Hydroxyl Groups in the Molecular Formula of Psr or Lpsr

The iron content of the analyzed spots of psr and lpsr is given as Fe_2O_3 wt % and not as FeO. In fact, it is detected that in the majority of the studied altered ilmenite grains, most of the iron content is present as ferric iron (Fe^{3+}). Considering that the psr formula is $\text{Fe}_2\text{Ti}_3(\text{O}_x, \text{OH}_y)$, where $x + y = 9$, the adopted procedure includes the following steps:

- The analyzed iron is given as Fe_2O_3 .
- The calculation of the molecular proportion for each analyzed oxide.
- The calculation of Ti-factor by dividing 3 by the calculated molecular proportion of the analyzed TiO_2 wt %.
- The calculation of the number of cations for each analyzed oxide by the normalization to 3 Ti (cation norm or cation mole %). Hence, the calculated molecular proportion of each oxide will be multiplied by the Ti-factor and also by the number of cations in its corresponding oxide formula.
- The calculation of cation norm sum except for Ti.
- The calculation of cation charge values sum (W1), except that of Ti. The cation charge value is calculated by multiplying each cation norm in cation charge inside its corresponding oxide.
- Now, in the psr formula of $\text{Fe}_2\text{Ti}_3(\text{O}_x + \text{OH}_y)$, the calculation of the number of oxygen and hydroxyl anions is calculated as follows: Because the number of positive charges must equal those of the negative charges, the sum of all cation charges except Ti + 12 (charges of 3Ti^{4+}) is equal to:

$$2X + Y \quad (5)$$

where:

$$X+Y=9. \text{ Then, } X = 9 - Y \quad (6)$$

Substituting the value of X of (6) in (5), we get:

$$\sum \text{all cation charges except Ti} + 12 = 2(9 - Y) + Y = 18 - Y$$

$$\text{Then, } \sum \text{all cation charge except Ti} + 12 = 18 - Y$$

$$\text{Then, } \sum \text{all cation charge except Ti} = 18 - 12 - Y$$

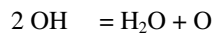
$$\text{Then, } Y = 6 - \sum \text{all cation charges except Ti} \quad (7)$$

- The calculation of OH wt % inside the psr formula ($\text{Fe}_2\text{Ti}_3\text{O}_x\text{OH}_y$), is:

$$\text{OH wt \%} = 17 \times Y \times 100 / \{(17 \times Y) + (16 \times X) + (3 \times 47.9) + W2\} \quad (8)$$

where the molecular weights of OH, O, and Ti are 17, 16, and 47.9, respectively, and W2 is the sum for each cation norm to 3Ti, except of Ti, multiplied by its atomic weight.

- The calculation of H_2O wt % is:



$$34.015 \text{ g} = 18.015 \text{ g}$$

Then, 100% OH gives 52.96 wt % H_2O .

Then, the H_2O wt % corresponding to the definite value of OH wt % is calculated as:

$$\text{H}_2\text{O wt \%} = \{\text{OH wt \%} \times 52.96\} / 100 \quad (9)$$

Substituting the value of OH wt % of (8) into (9), we get:

$$\text{H}_2\text{O wt \%} = Y \times 900.85 / (Y \times 17) + (X \times 16) + 143.7 + W2 \quad (10)$$

Applying this constructed psr and lpsr procedure for some of the spots under investigation, the calculated structural H_2O wt %, sometimes gets too high. The new calculated total oxide sums (N Total or NT), which include also the calculated structural water in the analyzed psr or lpsr spot, are much more than 100 wt %. The reason for such cases can be explained as follows:

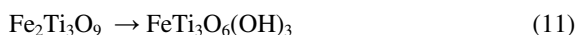
- If some of the analyzed TiO_2 wt % of a definite analyzed spot of psr is not included within the psr formula, it may be included in another associated individual mineral phase mixed with psr. In this case, the calculated value of Ti-cation proportion [TiO_2 wt % / molecular wt of TiO_2], will be relatively higher than that supposed to be actually present. Then, the calculated value of Ti-factor [3/the calculated Ti-cation proportion], will be relatively lower. Then, most of the calculated cation values, corresponding to the various analyzed cation oxides will be relatively lower when normalized by 3Ti. Hence, the calculated OH and the corresponding structural water wt % will be relatively higher. On the other hand, the presence of a definite portion of individual Fe_2O_3 with the analyzed amount of psr spot do not have the same effect as that of TiO_2 , and does not affect the calculated values of the other cations inside the psr formula structure.
- The presence of considerable contents of some elements, such as Mn^{2+} , that have charge of relatively lower value than Fe^{3+} , which decrease the sum value of (7). Hence, the

calculated values of Y and OH⁻ and the corresponding structural water wt % will be relatively higher.

- The presence of cations relatively lighter than iron and of charges ≥ 3 in considerable contents in the analyzed psr spot will affect the calculated value of Y, see (7). The reason is that their calculated cation proportions and their corresponding charges will be relatively higher and hence also the sum value of (7) will be. Then, the calculated values of Y and OH⁻ and the corresponding structural water wt % will be relatively lower.

2) The Second Method for Calculating the Number of Oxygen Anions (X) and the Number of Hydroxyl Groups (Y) in the Molecular Formula of Psr or Lpsr

In the lpsr stage, Fe³⁺ starts to leave the psr structure and hence oxygen must be also substituted or hydrogenated and replaced by OH⁻ anions. Then, the removal of each ferric iron cation will be associated with the substitution of three oxygen anions (3O²⁻) by three hydroxyl anions (3OH) to achieve the electrical neutralization and also to prevent the collapse of the psr structure. Then:



Then, in the structural molecular formula of lpsr:

Number of lost Fe³⁺ cations = $1/3 \times$ number of lost O²⁻ = $1/3 \times$ number of added or formed OH⁻

Hence, in the calculated lpsr formula, the difference of the present Fe³⁺ in the molecular formula from 2 must be multiplied by 3 to obtain the number of added or formed OH⁻ inside the lpsr molecular formula of the analyzed spot.

3) The Third Method for Calculating the Number of Oxygen Anions (X) and the Number of Hydroxyl Groups (Y) in the Molecular Formula of Psr or Lpsr

For a definite spot chemical analysis of psr or lpsr, when all the present analyzed cations are normalized to 3Ti, the calculated sum of oxygen anions is corresponding to the actual present cation positive charges in the psr molecular formula. Then, by multiplying the calculated number of oxygen anions by 2, the value of negative charges required to neutralize these positive charges is acquired. If the number of the calculated oxygen anions (O²⁻) is lower than 9, the number of OH⁻ anions present in the lpsr formula is obtained by multiplying the deficient value by 2. But because in the molecular formula of psr or lpsr, the number of O²⁻ anions plus the number of OH⁻ anions must be equal to 9, the correct number of O²⁻ anions in the lpsr formula equals to 9 minus the predicted number of OH⁻. For example, for a definite spot chemical analysis and if the number of the normalized calculated oxygen anions is equal to 7.5, then the predicted number of present OH⁻ anions is $9 - 7.5 = 1.5 \times 2 = 3$. But $\text{O}^{2-} + \text{OH}^{1-} = 9$. So, the correct occurred O²⁻ anions are $9 - 3 = 6$.

4) The Calculation of Lost Iron from the Formula Structure of Psr and Lpsr

There are two methods of calculating the lost iron from the psr and lpsr formula structure.

- Lost iron = the number of the calculated OH⁻ anions of psr or lpsr /3.
- Lost iron = 2- sum of all calculated cations in psr and lpsr with the exception of Ti.

When comparing the results of the different psr and lpsr analyzed spots using these two different methods for the calculation of lost iron (Fe³⁺), the following remarks can be concluded:

- In some analyzed spots, the calculated lost Fe³⁺ by the first method is relatively lower than that calculated by the second method. Some of the lost cations may be not be associated by the entrance of OH⁻ anions into the psr or lpsr formula structure or they are associated by the entrance of less OH⁻, i.e. two not three. For example, if one cation of Mg²⁺ or Mn²⁺, mixed with iron in the original ilmenite, is lost during alteration, then only two oxygen anions are replaced or changed with two OH⁻ anions inside the psr formula structure. In this case, the number of lost iron equals to the half, not third, of the number of OH⁻ anions. Hence, the calculated lost iron by the first method in this case is increased. Therefore, it was detected in the chemical analysis of some lpsr spots, that the difference of the calculated lost iron using these methods is more noticeable as the content of the analyzed MgO and/or MnO is relatively higher. In fact, many of the investigated lpsr spot chemical analysis containing TiO₂ ranging between 70 and 80 wt % have the calculated lost iron by the second method relatively greater than that calculated by the first one by values ranging between 0.07 and 0.2. The reason is that in this composition range of TiO₂, most of Mg²⁺, Mn²⁺ are mostly lost from the structure.
- On the other hand, in other analyzed spots, the calculated lost Fe³⁺ by the first method is relatively higher than that calculated by the second method. An amount of some analyzed oxides, hence their corresponding calculated cations, are not contained in the psr formula structure. They are mixed as impurities or as another mixed individual phase inside psr. Therefore, the calculated value of the total cations of the second method is increased and hence the lost iron is decreased.
- However, in a definite psr spot chemical analysis, all SiO₂, Al₂O₃, CaO, Na₂O, and K₂O are considered as impurities and must be neglected. Then, the other analyzed oxides must be multiplied by the factor:

$$100/100 - (\text{SiO}_2 + \text{Al}_2\text{O}_3 + \text{CaO} + \text{Na}_2\text{O} + \text{K}_2\text{O}) \quad (12)$$

to correct their values. In this case, the calculated iron by the first method is still more than that calculated by the second method with values ranging between 0.09 and 0.11. Then, some of the other analyzed oxides, such as MgO, MnO, ZnO, or Cr₂O₃ may be present as individual impurity phases not related to the content of iron contained in the psr.

C. Others

Stereoscopic binoculars and reflected-light polarizing microscopes were used. The heavy liquid separation technique was carried out for some investigated samples using Clerici's solution (sp. Gr.= 4.05). Jones ruffle splitters of various sizes were also used.

IV. RESULTS

The majority of the studied grains were obtained in the magnetic fractions of 0.1 and 0.2 A. They were composed mainly of fine hematite and ilmeno-hematite grains, some of magnetic primary rutile in addition to minor of altered ilmenite grains of elongated and spherical, rounded grains of highly pitted surfaces. They are mostly of black (Figure 1(1)) and dark brown (Figure 1(2)) colors.

The obtained magnetic fraction at 0.25 A is composed mainly of altered ilmenite varieties the same as those detected in the fractions at 0.1 and 0.2 A. They are black (Figure 1(1)) and dark brown (Figure 1(2)) grains with highly pitted surfaces. The black grains represent the 75 wt %, while the other variety the 25 wt % of the altered ilmenite grains in the fraction. The obtained magnetic fraction at 0.35 A is composed mainly of the same two altered ilmenite grains, black and dark brown. The brown grains (Figure 1(3)) are more abundant, coarser, and more rounded than the black ones. The relatively lighter brown, creamy, and yellowish brown colored grains (Figure 1(4)) are increased in the fraction. A considerable number of the black colored grains are stained to partially coated with relatively lighter opaque (dark brown, yellowish and reddish brown) colored soft material while the others are coated or stained with silica. The obtained magnetic fraction at 0.5 A is composed mainly of the black and brown altered ilmenite grains. The black grains are more abundant, angular, finer, and with highly pitted surfaces than the various brown grains. The grains of light brown, reddish and yellowish brown colors (Figure 1(5)) are highly increased in this fraction. The same characteristic stained and coated black grains are detected also within the black colored grains of the fraction. The obtained magnetic fraction at 1 A is composed of light brown, brownish yellow, and creamy colored grains (Figure 1(6)), in addition to minor black grains. Most grains are spherical, sub-rounded to well-rounded. The relatively coarser grains have highly pitted surfaces while the relatively finer ones have smooth surfaces. Some grains of the magnetic fraction at 1 A are separated as light fraction of Clerici's solution (sp. gr. = 4 g/cm³). The grains have several colored tints of pale brown, yellow, and creamy with highly pitted surfaces (Figure 1(7)). They contain a considerable number of the forementioned stained and coated grains. Several yellowish grains seem to be completely to partially coated with siliceous material. Some of these last grains were immersed in a solution of HF acid for 48 hours and then investigated under the binocular microscope. It was noticed that the coated materials for at least 50% of the grains are partially removed showing a core of highly pitted reddish, dark brown, and black rutile of vitreous luster (Figure 1(8)).

The obtained nonmagnetic fraction at 1 A is very close to the relatively heavier magnetic grains at 1 A, but they have relatively lighter colors. A chosen number of altered ilmenite

grains from each obtained magnetic fraction, giving a total of 84 grains including 586 determined spots, were investigated using the Cameca SX-100 EMPA. Also, a definite number of altered ilmenite grains from some of the obtained individual magnetic fractions were chosen and subjected to investigation using the XRD instrument.

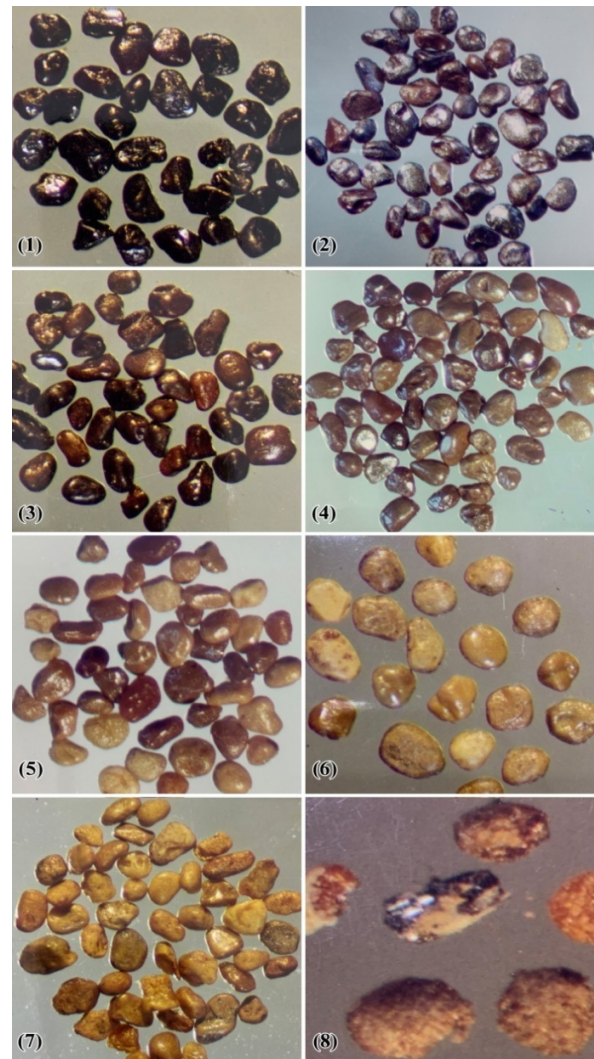


Fig. 1. The different leucoxenated altered ilmenite varieties: (1) The black and dark brownish black colored altered ilmenite varieties separated as magnetic at 0.1, 0.2, or 0.25 A. (2) The dark brown colored altered ilmenite varieties separated as magnetic at 0.1, 0.2 or 0.25 A. (3) The dark brown and brown colored altered ilmenite varieties separated as magnetic at 0.35 A. (4) The relatively lighter brown, creamy, and yellowish brown colored grains separated as magnetic at 0.35 A. (5) The grains of light brown, reddish and yellowish brown of highly pitted surfaces separated as magnetic at 0.50 A. (6) The light brown, brownish yellow, creamy and white grains separated as magnetic or as non-magnetic at 1 A. Most of the grains are spherical, sub-rounded to well rounded grains of highly pitted surfaces. (7) The pale brown, yellow, creamy, and white colored grains with highly pitted surfaces, separated as magnetic at 1 A. The grains are separated as a light fraction of Clerici's solution (sp. Gr. = 4 g/cm³). (8) The yellowish grains have completely to partially coatings of siliceous material after immersed in a solution of HF acid for 48 hours. The coated materials are partially removed showing a core of highly pitted reddish, dark brown and black rutile of vitreous luster. All images are acquired with a binocular microscope, X50.

V. DISCUSSION

A. The Separated Magnetic Fractions at 0.1 and 0.2 A

1) The Investigated Brown Colored Grains

Six brown grains were investigated. The investigated grains, the analyzed spots, their chemical analysis, and their corresponding molecular formulas are shown in Figure 2 and Table I.

The spots of the grain (Figure 2(1), Table I), are pseudorutile (psr) and leached pseudorutile (lpsr). The TiO_2 content ranges between 65.34 and 70.4 wt %, the Fe_2O_3 content between 30 and 19.59 wt %, and the $\text{Ti}/(\text{Ti}+\text{Fe})$ ratio between 0.64 and 0.75. Spots 1, 8, and 9 are individual inclusions. The inclusion size is relatively finer (spot 9), as the degree of the alteration gets relatively higher. Hence, spot 9 contains the highest TiO_2 content (70.4 wt %) and the lowest Fe_2O_3 content (19.59 wt %).

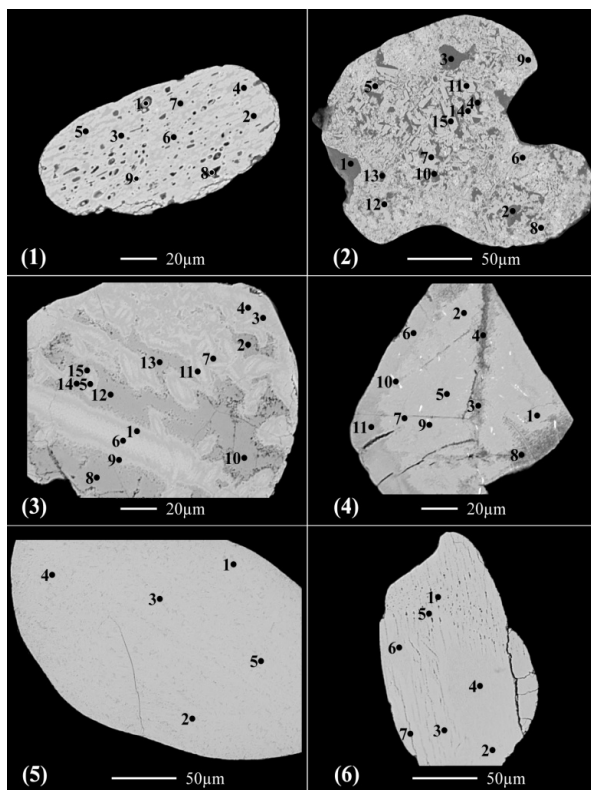


Fig. 2. The BSE images of the brown altered ilmenite grains, (1) to (6), separated as magnetic at 0.1 and 0.2 A.

In grain (2), the spots from 1 to 7 are a definite silicate mineral. Most of the constituent oxides of SiO_2 , Al_2O_3 , Fe_2O_3 , MgO , and K_2O are lost and an enrichment of the minor immobile TiO_2 is obtained. In the spots from 8 to 15, most of the two major oxides, SiO_2 and Al_2O_3 , of the altered silicate mineral are highly lowered and an individual TiO_2 bearing phase is formed, most probably a triple rutile phase (Figure 2(2)). Both spots 8 and 9 are located at the edges of the grain

and are relatively enriched with the leached Fe_2O_3 from the contained altered silicate mineral of the grain. It is obvious that spots 8, 9 seem falsely as lpsr (Table I). Some spots of altered silicate minerals can be falsely considered as psr or lpsr according to their chemical compositions. Therefore, BSE images of the analyzed spots and chemical composition analyses are at least required for the correct interpretation of such spots. It is obvious that the dependence on the powdered XRD analysis may be not enough to give correct decisions during the investigation of some analyzed grains related to psr and/or lpsr. The single crystal XRD may be a more efficient technique in such situations. Also, the investigation of the grains (1) and (2) reflects that some of the associated contained inclusions may be responsible for the acquired magnetic characteristics of some detected altered ilmenite grains.

Grains (3)-(6) (Figure 2, Table I), are psr and lpsr. In these grains, the TiO_2 content ranges between 62.23 and 78.09 wt %, the Fe_2O_3 content ranges between 33.21 and 14.47 wt %, and the $\text{Ti}/(\text{Ti}+\text{Fe})$ ratio ranges between 0.65 and 0.81. In grain (3), the content of TiO_2 increases as the contents of SiO_2 , Al_2O_3 , CaO , and structural water increase. On the other hand, the content of MnO follows the content of Fe_2O_3 . A comparison is made between the original total oxides sum (OT) and the new total oxides sum (NT). OT, in addition to the calculated H_2O wt % corresponding to structural water in the calculated chemical formula, reflects that the calculated structural water content for most of grain (3) spots is incorrect. In other words, not all the analyzed TiO_2 wt % of the spot are contained in the chemical formula of the lpsr phase. There are other phases of TiO_2 and are mixed with the lpsr phase. It is obvious that in the region of 68-70 TiO_2 wt % for the analyzed lpsr spots, the mechanism of ilmenite alteration may have changed. In grain (4), except of the spots 3, 4, and 8, the other spots consist of psr and lpsr. Spots 3 and 4 are located inside relatively larger cracks where the activity of molecular water seems to be high and hence the rate of alteration is relatively higher. When comparing the OT and NT, the existence of molecular water will be also assumed as the decrease of 100 wt % of the NT value (Table I). The values of the analyzed oxides must be recalculated and corrected by multiplying by $(100/\text{NT})$. In this case, all the obtained NT values are around 100 wt %. The same case is present with spot 8 which is located inside several cracks on the edge of grain (4). Hence, both TiO_2 and Fe_2O_3 contents in spots 3, 4, and 8 are relatively greater than those recorded (Table I). In these spots, which have obvious lower Fe_2O_3 content, the MnO content has relatively lower values. It is obvious that Fe_2O_3 and MnO contents are interdependent. Grains (5) and (6) are psr and lpsr. When comparing OT and NT, it is detected that the calculated structural water contents are incorrect, especially with spots that have relatively higher TiO_2 content. Hence, not all the analyzed TiO_2 values are contained within the psr phase, some individual TiO_2 -phases may exist in association with psr. This individual phase may be inherited from the originally altered ilmenite. Such explanation is obvious in grain (6) which seems as it was originally titanhematite-ferrilmenite exsolved intergrowth. Grain (5) may be ilmenite with some individual TiO_2 -phase content present in solid solution with ilmenite.

TABLE I. MICROPROBE CHEMICAL ANALYSES AND THE CORRESPONDING MOLECULAR FORMULAE OF THE ANALYZED SPOTS OF THE BROWN ALTERED ILMENITE GRAINS (1)-(6) OF FIGURE 2, SEPARATED AS MAGNETIC AT 0.1 AND 0.2 A

Grain	Spot	SiO ₂	MgO	MnO	CaO	ZnO	Fe ₂ O ₃	Al ₂ O ₃	Cr ₂ O ₃	Na ₂ O	K ₂ O	TiO ₂	OT	OH%	H ₂ O%	NT	Fe ₂	Ti ₃	Ox	OHy	Lost Fe	Ti/(Ti+Fe)
Fig. 2(1) 2b	1	1.82	0.70	0.62	0.19	0.00	29.22	0.73	0.05	0.02	0.04	63.73	97.13	4.63	2.45	99.58	1.66	3	7.98	1.02	0.34	0.64
	8	0.84	0.29	0.67	0.20	0.00	22.48	0.46	0.11	0.04	0.02	69.81	94.92	12.91	6.84	101.76	1.13	3	6.34	2.66	0.87	0.73
	9	0.90	0.30	0.59	0.26	0.00	19.59	0.55	0.11	0.06	0.03	70.40	92.78	14.97	7.93	100.71	1.00	3	5.98	3.02	1.00	0.75
Fig. 2(2)	8	8.69	0.25	0.13	0.32	0.00	9.76	7.31	0.11	0.06	0.10	70.13	96.85	5.86	3.11	99.96	1.47	3	7.82	1.18	0.53	
	9	7.97	0.47	0.10	0.37	0.00	4.76	5.56	0.07	0.07	0.26	71.56	91.18	12.30	6.51	97.69	1.10	3	6.64	2.36	0.90	
	10	10.71	0.26	0.00	0.21	0.00	3.12	6.69	0.06	0.04	0.10	76.95	98.14	11.04	5.84	103.99	1.13	3	6.89	2.11	0.87	
	11	7.84	0.10	0.01	0.21	0.00	1.44	5.71	0.04	0.06	0.06	80.36	95.83	17.43	9.23	105.06	0.81	3	5.77	3.23	1.19	
	12	7.78	0.24	0.09	0.35	0.00	3.88	5.17	0.09	0.05	0.08	80.87	98.58	16.14	8.55	107.13	0.88	3	5.97	3.03	1.12	
	13	5.13	0.07	0.04	0.11	0.00	2.20	3.51	0.04	0.06	0.03	88.72	99.90	23.52	12.45	112.35	0.51	3	4.74	4.26	1.49	
	14	3.87	0.07	0.00	0.23	0.00	1.67	2.63	0.05	0.05	0.05	89.74	98.37	26.13	13.84	112.21	0.39	3	4.31	4.69	1.61	
	15	0.66	0.01	0.04	0.02	0.00	1.08	0.41	0.04	0.00	0.01	97.94	100.20	32.79	17.37	117.57	0.08	3	3.28	5.72	1.92	
Fig. 2(3) 2d-2e	2	0.33	0.14	0.39	0.16	0.00	27.00	0.23	0.10	0.05	0.00	66.79	95.20	10.02	5.31	100.51	1.30	3	6.87	2.13	0.70	0.70
	3	0.35	0.18	0.56	0.21	0.00	26.95	0.27	0.13	0.02	0.01	68.10	96.77	10.23	5.42	102.18	1.29	3	6.83	2.17	0.71	0.70
	5	0.43	0.22	0.35	0.24	0.00	23.78	0.41	0.13	0.06	0.01	70.25	95.89	12.82	6.79	102.68	1.13	3	6.35	2.65	0.87	0.73
	13	0.90	0.25	0.11	0.43	0.00	15.97	0.72	0.21	0.11	0.06	76.37	95.13	18.76	9.94	105.07	0.79	3	5.34	3.66	1.21	0.79
Fig. 2(4)	15	0.90	0.19	0.05	0.47	0.00	14.63	0.74	0.22	0.09	0.04	78.09	95.42	20.08	10.64	106.06	0.72	3	5.13	3.87	1.28	0.81
	3	0.35	0.12	1.00	0.16	0.00	25.55	0.38	0.37	0.00	0.01	63.49	91.44	9.35	4.95	96.39	1.35	3	7.00	2.00	0.65	0.69
	4	0.43	0.12	0.82	0.19	0.00	24.16	0.49	0.42	0.03	0.01	63.94	90.59	10.34	5.47	96.07	1.29	3	6.82	2.18	0.71	0.70
Fig. 2(5)	8	0.65	0.16	0.84	0.23	0.00	18.82	0.59	0.42	0.04	0.03	65.68	87.45	14.38	7.62	95.07	1.04	3	6.08	2.92	0.96	0.74
	2	2.02	0.76	0.41	0.17	0.00	25.60	1.01	0.14	0.05	0.09	66.60	96.84	7.55	4.00	100.83	1.46	3	7.39	1.61	0.54	0.67
Fig. 2(6)	5	0.72	0.70	0.53	0.14	0.00	26.82	0.56	0.18	0.04	0.02	67.97	97.67	9.11	4.83	102.50	1.38	3	7.06	1.94	0.62	0.69
	1	0.40	0.25	1.23	0.19	0.00	23.85	0.72	0.14	0.05	0.04	67.05	93.92	11.10	5.88	99.80	1.25	3	6.67	2.33	0.75	0.71
	5	0.30	0.21	1.19	0.17	0.00	24.22	0.42	0.15	0.05	0.01	68.19	94.89	11.68	6.19	101.08	1.21	3	6.56	2.44	0.79	0.71
	7	0.28	0.19	1.16	0.21	0.00	22.03	0.64	0.16	0.07	0.02	70.56	95.32	13.64	7.22	102.55	1.10	3	6.20	2.80	0.90	0.73

The psr-lpsr of these investigated six grains have a chemical formula of Fe_{1.66-0.72}Ti₃O_{7.98-5.13}(OH)_{1.02-3.87} (Table I).

2) The Investigated Black Grains

Fourteen black grains are investigated. Except spot 1 of grain (7) (a definite silicate mineral), spot 1 of grain (16), spots 3, 4 of grain (18), spots 4, 5, 6 of grain (20) (leached ilmenite), and spot 5 of grain (17) (rutile and hematite), the rest spots of the grains (7)-(17) are composed of psr of various chemical formulas (Figure 3). The content of TiO₂ ranges between 57.5 and 73.71 wt %, the content of Fe₂O₃ between 37.98 and 19.34 wt %, and the Ti/(Ti+Fe) ratio between 0.60 and 0.74 (Table II). In spots 3-5 of grain (7), the comparison between OT and NT reflects that either the calculated structural water (OH), is incorrect or not all the analyzed TiO₂ content is included in the psr formula structure. Hence, some individual TiO₂-phases are mixed with the psr in the various analyzed spots of the grain. Grains (8)-10) are psr. In these grains, the content of TiO₂ and Fe₂O₃ and most of the other analyzed oxides seem to be homogeneous. Grain (11) seems that was originally titanhematite-ferrilmenite exsolved intergrowth where most of the titanhematite component was leached out while the ferrilmenite was altered to psr (spots 1-5). Spot 6 seems to be a mixture between TiO₂ and Fe₂O₃ phases and is not a psr phase. In this spot, OT equals to 98.8 wt %. If the remaining percentage (1.2 wt %) is totally structural water, it will be much lower and not accepted in a psr formula with such content of TiO₂ (68.8 wt %) and Fe₂O₃ (23.1 wt %). The analyzed value of MnO is another reason that spot 6 is not a psr phase where most of the analyzed altered ilmenite (spots 1-5) contain a definite amount of mixed pyrophanite component (up to 2.56 wt % MnO). In spot 6, there is a high decrease of the altered ilmenite component, and hence, the followed pyrophanite is reflected in its MnO content (1.2 MnO wt %).

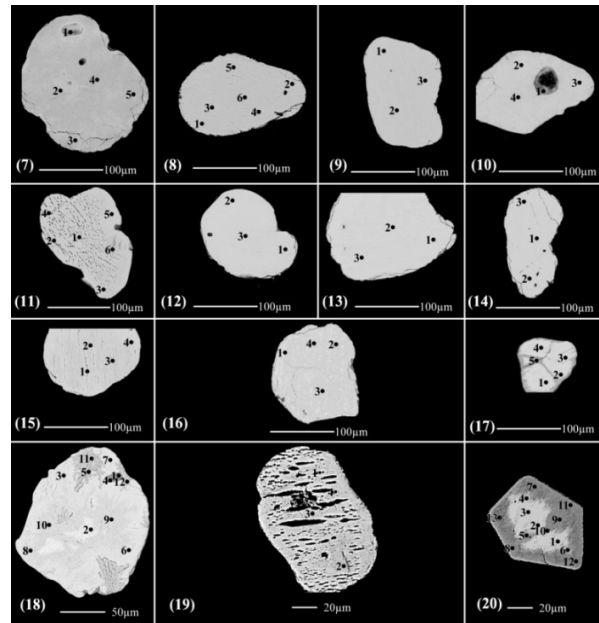


Fig. 3. BSE images of the black altered ilmenite grains (7)-(20), separated as magnetic at 0.1 and 0.2 A.

Grains (12), (13) are somewhat homogeneous psr. Grains (14)-(17) are psr (Figure 3, Table II). Grain (15) seems to be originally exsolved intergrowth of titanhematite-ferrilmenite. When comparing the OT and NT of the grain, either the calculated structural water is incorrect or not all the analyzed TiO₂ content is included in the psr chemical formula. Also, the recorded Al₂O₃ contents in grain (15) seem to be associated with the components of the original exsolved intergrowth. It may be most probably mixed with the titanhematite one. In

fact, grain (15), spreads light on some problems during the calculations of the various altered ilmenite phases. In much of the literature, the recorded SiO₂ and Al₂O₃ contents are considered as impurities and must be subtracted from the total oxide sum followed by the recalculation and correction of the other analyzed oxides. However, the most abundant analyzed oxide of the spot, TiO₂, will be highly affected by the

recalculation and correction. It increases with a relatively much more percentage than the other analyzed oxides, especially Fe₂O₃, the second major oxide of spot analysis. If SiO₂ and/or Al₂O₃ are not impurities, and are originally associated with only TiO₂ or with only Fe₂O₃ then, some misleading results will be obtained by considering these two oxides as impurities.

TABLE II. MICROPROBE CHEMICAL ANALYSES AND THE CORRESPONDING MOLECULAR FORMULAE OF THE ANALYZED SPOTS OF THE BLACK ALTERED ILMENITE GRAINS (7)-(20) OF FIGURE 3, SEPARATED AS MAGNETIC AT 0.1 AND 0.2 A

Grain	Spot	SiO ₂	MgO	MnO	CaO	ZnO	Fe ₂ O ₃	Al ₂ O ₃	Cr ₂ O ₃	Na ₂ O	K ₂ O	TiO ₂	OT	OH%	H ₂ O%	NT	Fe ₂	Ti ₃	Ox	OHy	Lost Fe	Ti/(Ti+Fe)
Fig. 3(7)	1	25.38	7.09	0.24	0.24	0.00	24.09	0.23	0.10	0.02	0.61	36.56	94.55	-46.53	-24.64	69.91	6.07	3	22.61	-13.61	-4.07	
	3	0.92	0.60	0.20	0.34	0.00	20.09	1.45	0.31	0.05	0.05	73.16	97.18	14.05	7.44	104.62	1.07	3	6.16	2.84	0.93	0.74
	5	0.90	0.56	0.26	0.34	0.00	20.49	1.49	0.32	0.03	0.04	72.98	97.40	13.73	7.27	104.68	1.08	3	6.21	2.79	0.92	0.73
Fig. 3(8)	1	0.15	1.77	0.55	0.04	0.00	33.46	0.09	0.02	0.01	0.01	61.22	97.32	2.66	1.41	98.73	1.87	3	8.40	0.60	0.13	0.62
	6	0.15	1.75	0.55	0.03	0.00	31.68	0.09	0.02	0.03	0.00	62.25	96.55	4.27	2.26	98.81	1.75	3	8.04	0.96	0.25	0.63
Fig. 3(9)	1	0.15	2.42	0.54	0.10	0.00	34.14	0.10	0.03	0.04	0.02	59.69	97.23	0.95	0.50	97.73	2.02	3	8.78	0.22	-0.02	0.60
	3	0.16	2.20	0.51	0.07	0.00	33.65	0.07	0.02	0.01	0.03	60.57	97.29	1.90	1.01	98.29	1.94	3	8.57	0.43	0.06	0.61
Fig. 3(10)	1	0.22	0.21	0.60	0.20	0.00	29.10	0.98	0.08	0.00	0.01	60.90	92.30	5.74	3.04	95.34	1.60	3	7.73	1.27	0.40	0.65
	4	0.39	0.12	0.43	0.18	0.00	29.73	0.25	0.11	0.07	0.01	65.86	97.14	7.72	4.09	101.23	1.45	3	7.33	1.67	0.55	0.67
Fig. 3(11)	1	0.24	0.10	2.38	0.16	0.00	31.70	0.35	0.09	0.05	0.02	57.50	92.57	2.35	1.24	93.82	1.87	3	8.46	0.54	0.13	0.62
	2	0.22	0.07	1.92	0.09	0.00	35.95	0.32	0.10	0.03	0.00	60.19	98.89	0.98	0.52	99.41	1.96	3	8.77	0.23	0.04	0.60
	6	2.86	0.24	1.20	0.11	0.00	23.09	2.22	0.13	0.04	0.07	68.79	98.75	7.86	4.16	102.91	1.43	3	7.34	1.66	0.57	0.68
Fig. 3(12)	3	0.24	1.54	0.37	0.07	0.00	32.20	0.31	0.39	0.01	0.01	64.21	99.34	4.33	2.30	101.63	1.73	3	8.03	0.97	0.27	0.63
Fig. 3(13)	3	0.31	0.13	1.53	0.17	0.00	30.65	0.27	0.14	0.02	0.01	62.51	95.73	5.44	2.88	98.61	1.63	3	7.79	1.21	0.37	0.65
Fig. 3(14)	3	0.29	0.13	1.45	0.14	0.00	29.09	0.33	0.10	0.03	0.02	67.84	99.43	8.32	4.41	103.83	1.43	3	7.20	1.80	0.57	0.68
Fig. 3(15)	3	0.40	0.10	0.41	0.17	0.00	28.09	1.14	0.29	0.03	0.02	67.45	98.11	8.35	4.42	102.53	1.41	3	7.21	1.79	0.59	0.68
	4	0.38	0.10	0.63	0.18	0.00	26.11	1.23	0.27	0.04	0.02	68.89	97.85	9.95	5.27	103.12	1.31	3	6.90	2.10	0.69	0.70
Fig. 3(16)	1	0.09	0.14	2.28	0.06	0.00	38.21	0.00	0.05	0.03	0.00	59.19	100.04	-0.60	-0.32	99.72	2.10	3	9.14	-0.14	-0.10	
	4	0.46	0.07	0.32	0.19	0.00	31.10	0.17	0.11	0.02	0.01	65.07	97.51	6.66	3.52	101.04	1.52	3	7.54	1.46	0.48	0.66
Fig. 3(17)	4	0.15	0.38	0.97	0.07	0.00	34.49	0.03	0.09	0.06	0.01	61.25	97.49	2.96	1.57	99.06	1.81	3	8.33	0.67	0.19	0.62
	5	3.24	0.21	0.07	0.86	0.00	6.21	0.73	0.16	0.18	0.03	78.31	90.00	23.38	12.38	102.38	0.54	3	4.68	4.32	1.46	0.85
Fig. 3(18)	1	47.83	5.59	0.02	0.30	0.00	13.20	13.92	0.06	0.11	3.23	4.38	88.62	-176.16	-93.30	-4.67	79.49	3	269.27	-260.27	-77.49	
	2	0.00	0.07	1.90	0.02	0.00	52.94	0.00	0.00	0.02	0.01	47.51	102.46	-15.39	-8.15	94.31	3.49	3	13.33	-4.33	-1.49	
	3	0.31	0.13	1.67	0.07	0.00	37.33	0.15	0.02	0.05	0.03	57.45	97.21	-0.93	-0.49	96.72	2.11	3	9.22	-0.22	-0.11	
	4	0.15	0.08	1.80	0.03	0.00	38.73	0.05	0.02	0.00	0.02	57.88	98.75	-1.30	-0.69	98.06	2.14	3	9.31	-0.31	-0.14	
	5	0.92	0.34	0.96	0.19	0.00	28.85	0.78	0.11	0.02	0.04	58.12	90.33	3.83	2.03	92.35	1.73	3	8.14	0.86	0.27	0.63
	6	0.10	0.10	1.14	0.05	0.00	37.76	0.05	0.02	0.00	0.03	59.01	98.26	0.15	0.08	98.34	2.01	3	8.96	0.04	-0.01	0.60
	7	0.12	0.08	1.35	0.04	0.00	36.42	0.05	0.04	0.04	0.01	59.34	97.49	1.04	0.55	98.04	1.95	3	8.76	0.24	0.05	0.61
	8	0.32	0.15	1.04	0.11	0.00	31.87	0.12	0.03	0.02	0.03	62.83	96.51	5.22	2.76	99.27	1.63	3	7.84	1.16	0.37	0.65
	9	0.42	0.11	2.07	0.17	0.00	25.70	0.19	0.02	0.06	0.04	67.88	96.65	10.33	5.47	102.12	1.31	3	6.81	2.19	0.69	0.70
	10	0.43	0.16	1.56	0.16	0.00	24.29	0.19	0.03	0.08	0.02	69.86	96.78	12.09	6.40	103.18	1.19	3	6.48	2.52	0.81	0.72
	11	1.12	0.37	0.31	0.24	0.00	12.16	0.98	0.15	0.08	0.04	72.83	88.27	20.43	10.82	99.09	0.70	3	5.09	3.91	1.30	0.81
	12	1.69	0.51	0.21	0.32	0.00	12.36	0.91	0.12	0.07	0.09	73.96	90.24	19.73	10.45	100.69	0.74	3	5.21	3.79	1.26	0.80
Fig. 3(19)	1	0.18	0.09	1.77	0.16	0.02	28.27	0.15	0.10	0.00	0.00	55.61	86.34	4.71	2.50	88.83	1.69	3	7.94	1.06	0.31	0.64
	4	0.22	0.18	1.44	0.12	0.14	30.29	0.21	0.05	0.00	0.00	64.10	96.75	6.46	3.42	100.17	1.56	3	7.58	1.42	0.44	0.66
Fig. 3(20)	1	0.00	0.15	2.31	0.00	0.16	48.58	0.00	0.00	0.00	0.00	49.90	101.11	-11.64	-6.17	94.95	3.11	3	12.13	-3.13	-1.11	
	2	0.00	0.18	2.12	0.02	0.20	49.25	0.00	0.00	0.00	0.00	50.32	102.09	-11.75	-6.22	95.86	3.11	3	12.16	-3.16	-1.11	
	6	0.00	0.19	1.79	0.02	0.07	43.96	0.00	0.00	0.00	0.00	52.76	98.79	-7.00	-3.71	95.08	2.64	3	10.78	-1.78	-0.64	
	8	0.06	0.16	0.98	0.03	0.02	33.33	0.05	0.03	0.00	0.00	57.27	91.92	2.49	1.32	93.24	1.83	3	8.43	0.57	0.17	0.62
	12	0.02	0.22	0.56	0.05	0.04	33.28	0.06	0.00	0.00	0.00	58.40	92.61	3.22	1.70	94.32	1.78	3	8.27	0.73	0.22	0.63
13	0.12	0.24	0.48	0.07	0.03	30.70	0.09	0.02	0.00	0.00	60.82	92.57	5.81	3.08	95.65	1.59	3	7.71	1.29	0.41	0.65	

Grain (16) seems that was originally titanhematite-ferrilmenite exsolved intergrowth. Some of the remaining individual components of minor TiO₂ and/or minor Fe₂O₃ may be still mixed with the formed psr after the ilmenite alteration. In grain (17), because spot 5 is in a crack, the rate of alteration is relatively higher than those of the other spots due to the increased water activity bearing for SiO₂, Al₂O₃, and maybe CaO. Hence, the leaching of the contained Fe₂O₃ from the psr is highly increased and another lpsr phase is attained which

may be followed by the collapse into two individual phases for TiO₂ and Fe₂O₃. In grain (18), spot 1 is a definite silicate mineral. Spot 2 is most probably ferrilmenite. Spots 3 and 4 are leached ilmenite. When comparing OT and NT, spot 5 contains a relatively higher content of molecular water (Table II). From the OT value, both structural and molecular water types reach 9.7 wt %, while from the NT value the structural water is 2.03 wt %. The content of molecular water almost equals to 7.66 wt %. If the values of TiO₂ and Fe₂O₃ are

corrected by multiplying by (100/92.35), then they become 62.95 and 31.25 wt %, respectively. Then, spot 5 will have a composition like that of spot 8 (Table II). Also, in grain (18), it is obvious that the content of molecular water increases as the contents of the associated SiO_2 and Al_2O_3 increase (Table II). Spots 6-8 are psr with Ti/Ti+Fe ratio ranges between 0.6 and 0.65. According to the NT values, the spots 9 and 10 are psr mixed with minor TiO_2 and/or Fe_2O_3 individual phases. The Ti/Ti+Fe ratio ranges between 0.7 and 0.72. Spots 11 and 12 are lpsr of different chemical formulas. Their Ti/Ti+Fe ratio ranges between 0.8 and 0.81. The MnO content in these two spots is highly lowered due to the decrease of the corresponding Fe_2O_3 content which insures the direct relation between Fe_2O_3 and MnO. Also, the investigation of spots 11 and 12 insures that as the content of structural water contained in the lpsr phase increases, the associated SiO_2 and/or Al_2O_3 contents also increase. Grain (19) is originally exsolved intergrowth of titanhematite-ferrilmenite. Most of the hematite component is leached out and the associated ilmenite component is altered to psr. Spot 1 is psr associated with a considerable amount of molecular water reaching a value of 11.17 wt % (Table II). In grain (20), the spots 1-3 are ilmenite. Spots 4-6 are leached ilmenite and spots 7-13 are psr. It is noticed that spots 7-13 contain a considerable amount of molecular water which reflects the role of water in the initial alteration stages of ilmenite alteration. The psr-lpsr of these investigated grains have the chemical formula range of $\text{Fe}_{2.02-0.54}\text{Ti}_{3.08-4.68}(\text{OH})_{0.22-4.32}$ (Table II). Only 3 spots have Fe content ranging between 2.01 and 2.02 due to the appreciable contents of Mg^{2+} and/or Mn^{2+} which have relatively lower oxidation states than Fe^{3+} .

B. The Separated Magnetic Fraction at 0.25 A

Twenty one opaque brown grains and 18 black grains were investigated.

1) The Investigated Brown Grains

Most of the analyzed spots of the grains (Figure 4, Table III) are composed of psr and lpsr whereas the spots 1-5 in grain (1) and the spots 2 and 5 in grain (2) are leached ilmenite (Table III). In psr and lpsr analyzed spots, the TiO_2 content ranges between 57.63 and 69.79 wt %, the Fe_2O_3 content between 20.97 and 37.27 wt %, and the Ti/Ti+Fe ratio between 0.6 and 0.75. In the grain (3) of Figure 4, spots 1 and 2 contain a considerable amount of molecular water (Table III). The molecular water may have reached 16.6 wt % in spot 1 which is located at the edge of the grain while it reaches 10.3 wt % in spot 2 which is located beside several pores of a preexisting leached titanhematite. Also, in spot 1 of grains (4) and (5), the contained molecular water is relatively higher and attains 8.8 and 16.38 wt %, respectively (Table III). In fact, most of the spots having an appreciable content of molecular water (spots 1 and 2 in (3), spot 1 in (4), and spot 1 in (5)), also contain relatively higher contents of SiO_2 and Al_2O_3 . This may indicate the ability of these two oxides of bearing molecular water or OH^- anions.

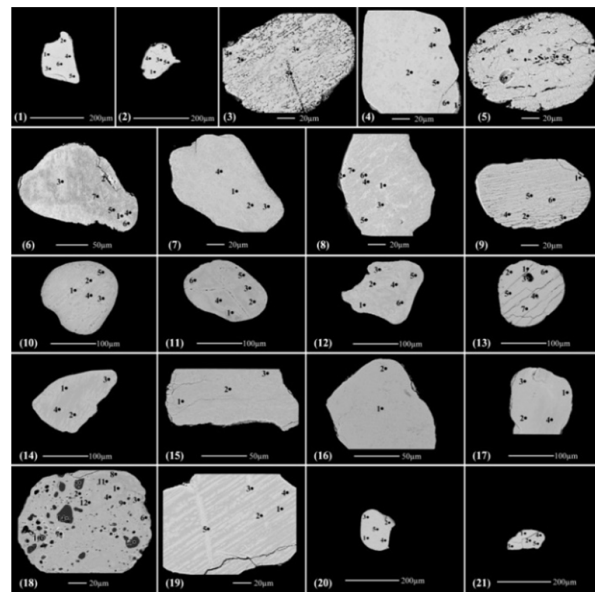


Fig. 4. BSE images of the brown altered ilmenite grains (1)-(21), separated as magnetic at 0.25 A.

Grains (6)-(9) in Figure 4, are composed of psr. Also, most of the analyzed spots of these four grains contain definite amounts of molecular water. The comparison of the values of OT and NT (Table III) reflects the occurrence of some molecular water. Both grains (10) and (11) are psr of various chemical formulas. In these two grains, the content of structural and/or molecular water is increased, as the analyzed zones are relatively darker. Grains (12) and (13) are psr. Spot 1 of grain (13) is in a location of a preexisting leached titanhematite, hence there is a definite content of molecular water (Table III). However, these grains show that the presence of preexisting leached phases bearing for TiO_2 affects the calculation of the NT of the detected psr chemical formulas, since it exceeds 100 wt %. In the rest 8 investigated grains, (14)-(21) (Figure 4 and Table III), except spot 5 (mixture of silica and psr), and spots 13 and 14 (silica) of grain (18), all the other investigated grains are psr and lpsr with TiO_2 content ranging between 64.77 and 76.35 wt %, Fe_2O_3 content ranging between 12.24 and 28.96 wt %, and Ti/Ti+Fe ratio ranging between 0.67 and 0.79.

In spots 3 and 4 of grain (14), the content of Fe_2O_3 becomes relatively lower, as the contents of SiO_2 , Al_2O_3 , Cr_2O_3 , and CaO become relatively higher while the contents of MgO and MnO become relatively lower. The increment of SiO_2 and Al_2O_3 contents seems to be correlated with the enrichment of TiO_2 content which correlates directly with the contained structural water of the formed lpsr phase. However, the NT of the spots 3 and 4 is much more than 100 wt %. Then, either the calculated structural water is incorrect or not all the analyzed TiO_2 content is included within the lpsr phase formula. Such TiO_2 content may be preexisting as a solid solution with the original ilmenite or is individually separated outside the lpsr phase structure at a definite alteration stage. The same situation is also recorded in the spots of grains (17)-(21), especially when the content of TiO_2 exceeds the value 68 or 69 wt %. Grains (15) and (16) are lpsr. Except spots 13 and 14 of grain (18), the other analyzed spots are composed of lpsr. Also, spots

7-12 have the same remarks explained with spots 3-4 of grain (14). The psr-lpsr of these investigated grains have the chemical formula range of $Fe_{2.03-0.81}Ti_3O_{9-5.4}(OH)_{0-3.6}$ (Table III). Only 2 spot analyses have Fe content ranging between 2.01 and 2.03 due to the appreciable contents of Mn and/or Mg which have oxidation state of 2⁺.

2) The Investigated Black Grains

Except spots 1-4 of grain (34), spots 1-8, and 10 of grain (35), and spots 1, 2 of grain (37) which are leached ilmenite, all the other spots of grains (22)-(39) (Figure 5, Table IV), are composed of psr. The TiO₂ content ranges between 58.05 and

63.34 wt %, the Fe₂O₃ content between 37.7 and 26.96 wt %, and the Ti/Ti+Fe ratio between 0.60 and 0.67. In spot 7 of grain (27), it is difficult to accept that the OT is 96.86 wt % and that NT equals to 111.97 wt % (Table IV). The value of the analyzed Fe₂O₃ equals to 2.44 wt %. In fact, the lpsr of this spot is broken into individual phases of TiO₂ and Fe₂O₃ where most of the contained Fe₂O₃ is leached out. Both SiO₂ and Al₂O₃ contents in this spot are relatively much higher than those of the other spots. However, there is a considerable amount of molecular water in the spot, which reaches 3.14 wt % (100 wt % - 96.86 wt %). Both SiO₂ and Al₂O₃ may be related to the associated molecular water.

TABLE III. MICROPROBE CHEMICAL ANALYSES AND THE CORRESPONDING MOLECULAR FORMULAE OF THE ANALYZED SPOTS OF THE BROWN ALTERED ILMENITE GRAINS (1)-(21) OF FIGURE 4, SEPARATED AS MAGNETIC AT 0.25 A

Grain	Spot	SiO ₂	MgO	MnO	CaO	ZnO	Fe ₂ O ₃	Al ₂ O ₃	Cr ₂ O ₃	Na ₂ O	K ₂ O	TiO ₂	OT	OH%	H ₂ O%	NT	Fe ₂	Ti ₃	Ox	OHy	Lost Fe	Ti/(Ti+Fe)
Fig. 4(1)	1	0.18	0.60	0.53	0.06	0.10	39.94	0.10	0.06	0.00	0.01	57.78	99.36	-2.13	-1.13	98.23	2.20	3	9.51	-0.51	-0.20	
	6	0.11	0.70	0.71	0.09	0.03	35.41	0.09	0.04	0.00	0.02	60.09	97.29	1.75	0.93	98.21	1.90	3	8.60	0.40	0.10	0.61
Fig. 4(2)	2	0.09	0.45	1.02	0.10	0.14	37.61	0.06	0.07	0.00	0.00	58.06	97.60	-0.52	-0.27	97.32	2.08	3	9.12	-0.12	-0.08	
	5	0.06	0.63	0.91	0.06	0.00	37.46	0.03	0.03	0.03	0.01	58.57	97.77	-0.12	-0.07	97.71	2.05	3	9.03	-0.03	-0.05	
Fig. 4(3)	1	2.85	0.14	0.25	0.17	0.00	28.70	2.16	0.05	0.05	0.21	48.82	83.39	-4.18	-2.22	81.18	2.29	3	9.99	-0.99	-0.29	
	2	0.73	0.20	0.16	0.10	0.00	31.56	0.16	0.00	0.01	0.03	56.71	89.66	2.94	1.56	91.22	1.78	3	8.33	0.67	0.22	0.63
Fig. 4(4)	1	0.60	0.77	0.61	0.12	0.00	29.88	0.76	0.09	0.01	0.04	56.82	89.72	2.81	1.49	91.21	1.82	3	8.37	0.63	0.18	0.62
	6	0.18	1.78	0.43	0.14	0.00	28.98	0.33	0.08	0.00	0.00	62.00	93.93	5.68	3.01	96.94	1.65	3	7.75	1.25	0.35	0.65
Fig. 4(5)	1	2.21	0.27	1.11	0.13	0.06	28.15	0.68	0.04	0.00	0.05	50.93	83.62	-0.47	-0.25	83.37	2.02	3	9.11	-0.11	-0.02	
	6	0.02	0.02	0.64	0.09	0.09	22.91	1.16	0.03	0.00	0.02	62.10	87.06	11.01	5.83	92.90	1.25	3	6.69	2.31	0.75	0.71
Fig. 4(6)	1	0.32	0.19	2.01	0.15	0.03	31.97	0.26	0.21	0.01	0.02	59.98	95.14	3.23	1.71	96.84	1.80	3	8.27	0.73	0.20	0.63
	7	0.60	0.19	1.74	0.20	0.00	26.20	0.40	0.19	0.04	0.01	65.02	94.60	8.67	4.59	99.19	1.41	3	7.14	1.86	0.59	0.68
Fig. 4(7)	1	0.18	1.17	0.37	0.12	0.00	31.09	0.18	0.15	0.00	0.01	59.85	93.11	4.09	2.17	95.28	1.74	3	8.08	0.92	0.26	0.63
	4	0.21	1.06	0.34	0.15	0.10	30.25	0.22	0.14	0.00	0.00	61.41	93.88	5.26	2.79	96.66	1.65	3	7.83	1.17	0.35	0.64
Fig. 4(8)	1	0.12	0.09	1.21	0.07	0.13	33.00	0.06	0.06	0.05	0.02	60.21	95.03	3.63	1.92	96.95	1.76	3	8.18	0.82	0.24	0.63
	7	0.27	0.10	0.82	0.13	0.11	29.07	0.31	0.04	0.02	0.03	62.89	93.78	7.13	3.77	97.55	1.50	3	7.44	1.56	0.50	0.67
Fig. 4(9)	1	0.36	0.12	0.99	0.23	0.05	25.54	0.54	0.00	0.00	0.03	62.86	90.72	9.18	4.86	95.58	1.37	3	7.04	1.96	0.63	0.69
	6	0.39	0.11	1.13	0.24	0.16	23.72	0.31	0.02	0.05	0.02	66.81	92.95	11.75	6.22	99.18	1.21	3	6.54	2.46	0.79	0.71
Fig. 4(10)	1	0.23	0.06	0.95	0.10	0.00	33.01	0.32	0.09	0.01	0.03	62.67	97.46	4.39	2.32	99.78	1.69	3	8.01	0.99	0.31	0.64
	5	0.53	0.13	0.38	0.23	0.00	24.17	0.87	0.23	0.09	0.01	68.13	94.77	11.36	6.01	100.79	1.22	3	6.63	2.37	0.78	0.71
Fig. 4(11)	1	0.37	0.07	0.35	0.17	0.00	22.92	0.39	0.16	0.02	0.00	64.95	89.39	12.29	6.51	95.90	1.16	3	6.45	2.55	0.84	0.72
	5	0.36	0.06	0.33	0.14	0.00	20.97	0.42	0.16	0.04	0.00	67.71	90.18	14.51	7.69	97.86	1.02	3	6.05	2.95	0.98	0.75
Fig. 4(12)	1	0.70	0.15	1.19	0.16	0.00	31.43	0.51	0.11	0.01	0.01	62.83	97.08	4.53	2.40	99.48	1.68	3	7.99	1.01	0.32	0.64
	6	0.49	0.21	0.96	0.24	0.00	23.90	0.44	0.21	0.04	0.02	69.37	95.87	12.03	6.37	102.24	1.19	3	6.50	2.50	0.81	0.72
Fig. 4(13)	1	0.67	0.17	0.45	0.25	0.00	23.00	1.39	0.15	0.11	0.15	60.20	86.54	8.87	4.70	91.24	1.39	3	7.11	1.89	0.61	0.68
	7	0.42	0.24	0.43	0.20	0.00	24.69	0.59	0.19	0.02	0.02	69.79	96.59	11.83	6.26	102.86	1.19	3	6.54	2.46	0.81	0.72
Fig. 4(14)	3	0.77	0.44	0.21	0.33	0.00	19.67	0.38	0.18	0.01	0.04	74.38	96.40	16.16	8.56	104.96	0.93	3	5.77	3.23	1.07	0.76
	4	0.87	0.30	0.23	0.42	0.00	17.03	0.43	0.23	0.04	0.04	77.09	96.68	18.40	9.74	106.42	0.81	3	5.40	3.60	1.19	0.79
Fig. 4(15)	3	2.37	0.96	0.33	0.22	0.00	21.83	1.01	0.21	0.05	0.17	68.60	95.75	10.11	5.36	101.10	1.30	3	6.90	2.10	0.70	0.70
Fig. 4(16)	2	1.75	1.08	0.38	0.13	0.00	21.77	0.75	0.18	0.04	0.14	68.35	94.57	11.04	5.85	100.42	1.25	3	6.71	2.29	0.75	0.71
Fig. 4(17)	1	0.34	0.15	0.55	0.15	0.00	26.54	0.32	0.09	0.00	0.03	68.08	96.24	10.57	5.60	101.84	1.27	3	6.77	2.23	0.73	0.70
	3	0.46	0.15	0.38	0.21	0.00	22.81	0.40	0.13	0.06	0.02	71.15	95.78	13.77	7.30	103.07	1.07	3	6.18	2.82	0.93	0.74
Fig. 4(18)	1	0.43	0.12	0.13	0.28	0.00	26.64	0.19	0.05	0.07	0.02	66.78	94.70	10.31	5.46	100.16	1.28	3	6.82	2.18	0.72	0.70
	4	0.41	0.10	0.17	0.26	0.00	25.71	0.22	0.07	0.07	0.02	67.57	94.59	11.18	5.92	100.51	1.23	3	6.65	2.35	0.77	0.71
	5	6.60	0.14	0.17	0.29	0.00	21.47	0.31	0.08	0.07	0.02	68.39	97.54	7.05	3.73	101.28	1.40	3	7.53	1.47	0.60	0.68
	7	0.61	0.16	0.23	0.29	0.00	23.39	0.36	0.10	0.07	0.04	69.39	94.64	12.81	6.79	101.42	1.13	3	6.36	2.64	0.87	0.73
	8	0.50	0.14	0.11	0.35	0.00	21.01	0.30	0.10	0.02	0.02	71.65	94.21	15.35	8.13	102.34	0.97	3	5.90	3.10	1.03	0.75
	10	0.59	0.15	0.14	0.33	0.00	20.20	0.35	0.15	0.05	0.04	72.56	94.56	15.91	8.42	102.99	0.94	3	5.81	3.19	1.06	0.76
	12	0.59	0.17	0.15	0.33	0.00	21.16	0.42	0.14	0.04	0.04	72.76	95.79	15.19	8.04	103.83	0.98	3	5.93	3.07	1.02	0.75
	13	97.88	0.00	0.00	0.02	0.00	0.35	0.00	0.01	0.00	0.03	0.73	99.02	-273.98	-145.10	-46.08	539.47	3	2158.49	-2149.49	-537.47	
	14	97.38	0.02	0.00	0.04	0.00	0.35	0.17	0.00	0.01	0.04	0.80	98.80	-273.04	-144.60	-45.80	490.84	3	1962.36	-1953.36	-488.84	
	Fig. 4(19)	1	0.42	0.16	0.54	0.29	0.08	21.94	0.52	0.10	0.01	0.03	69.00	93.09	13.62	7.21	100.31	1.08	3	6.21	2.79	0.92
5		0.62	0.19	0.35	0.40	0.02	18.11	0.69	0.08	0.03	0.01	72.49	92.99	16.88	8.94	101.93	0.89	3	5.65	3.35	1.11	0.77
Fig. 4(20)	1	0.38	0.51	1.22	0.24	0.00	23.73	0.50	0.11	0.05	0.02	69.40	96.16	11.87	6.29	102.45	1.21	3	6.53	2.47	0.79	0.71
	5	0.40	0.53	1.12	0.23	0.03	21.82	0.52	0.09	0.04	0.02	71.53	96.33	13.77	7.30	103.63	1.09	3	6.18	2.82	0.91	0.73
Fig. 4(21)	1	1.07	0.30	0.23	0.38	0.00	19.64	1.09	0.23	0.04	0.04	74.22	97.22	15.11	8.00	105.23	0.99	3	5.97	3.03	1.01	0.75
	5	1.14	0.22	0.18	0.43	0.04	16.94	1.29	0.33	0.02	0.02	76.35	96.96	17.17	9.09	106.06	0.87	3	5.62	3.38	1.13	0.77

TABLE IV. MICROPROBE CHEMICAL ANALYSES AND THE CORRESPONDING MOLECULAR FORMULAE OF THE ANALYZED SPOTS OF THE BLACK ALTERED ILMENITE GRAINS (22)-(39) OF FIGURE 5, SEPARATED AS MAGNETIC AT 0.25 A

Grain	Spot	SiO ₂	MgO	MnO	CaO	ZnO	Fe ₂ O ₃	Al ₂ O ₃	Cr ₂ O ₃	Na ₂ O	K ₂ O	TiO ₂	OT	OH %	H ₂ O %	NT	Fe ₂	Ti ₃	Ox	OHy	Lost Fe	Ti/(Ti+Fe)
Fig. 5(22)	1	0.20	0.02	1.27	0.10	0.00	32.46	0.18	0.10	0.01	0.00	59.68	94.01	3.66	1.94	95.95	1.75	3	8.17	0.83	0.25	0.63
Fig. 5(23)	1	0.23	0.12	0.60	0.12	0.00	32.72	0.12	0.04	0.00	0.01	60.98	94.95	4.30	2.28	97.23	1.69	3	8.03	0.97	0.31	0.64
	5	0.21	0.10	0.57	0.10	0.02	31.87	0.10	0.07	0.04	0.01	61.95	95.05	5.29	2.80	97.85	1.62	3	7.82	1.18	0.38	0.65
Fig. 5(24)	4	0.55	0.16	1.17	0.16	0.46	26.96	0.32	0.11	0.06	0.01	63.34	93.30	7.92	4.19	97.49	1.46	3	7.28	1.72	0.54	0.67
Fig. 5(25)	1	0.12	0.08	0.93	0.07	0.03	37.48	0.09	0.10	0.00	0.00	59.19	98.08	0.41	0.22	98.29	1.99	3	8.90	0.10	0.01	0.60
Fig. 5(26)	3	0.18	0.10	0.88	0.12	0.08	32.16	0.16	0.01	0.01	0.01	63.14	96.83	5.38	2.85	99.67	1.62	3	7.80	1.20	0.38	0.65
Fig. 5(27)	6	0.10	0.05	5.55	0.04	0.00	31.32	0.00	0.03	0.01	0.00	60.92	98.03	3.07	1.62	99.65	1.87	3	8.29	0.71	0.13	0.62
	7	1.60	0.14	0.10	0.71	0.00	2.44	1.62	0.17	0.07	0.04	89.98	96.86	28.53	15.11	111.97	0.30	3	3.90	5.10	1.70	
Fig. 5(28)	2	0.70	0.19	2.52	0.07	0.03	34.36	0.32	0.17	0.02	0.03	59.99	98.40	0.92	0.49	98.89	1.97	3	8.79	0.21	0.03	0.60
	5	0.20	0.08	2.94	0.07	0.09	32.99	0.08	0.10	0.03	0.02	61.62	98.23	3.21	1.70	99.93	1.81	3	8.27	0.73	0.19	0.62
Fig. 5(29)	1	0.10	0.28	0.62	0.13	0.01	35.40	0.16	0.05	0.00	0.01	60.61	97.36	2.31	1.22	98.58	1.85	3	8.47	0.53	0.15	0.62
	5	0.08	0.25	0.80	0.11	0.03	33.42	0.13	0.03	0.01	0.00	62.73	97.58	4.45	2.36	99.94	1.69	3	8.00	1.00	0.31	0.64
Fig. 5(30)	1	0.79	0.09	1.40	0.18	0.00	35.23	0.27	0.06	0.00	0.02	59.76	97.80	0.88	0.47	98.27	1.95	3	8.80	0.20	0.05	0.61
	5	0.71	0.10	1.18	0.21	0.00	32.77	0.30	0.08	0.02	0.02	63.26	98.65	4.00	2.12	100.77	1.72	3	8.10	0.90	0.28	0.64
Fig. 5(31)	1	0.12	0.13	1.35	0.09	0.10	36.30	0.11	0.06	0.04	0.01	60.30	98.60	1.33	0.70	99.30	1.93	3	8.69	0.31	0.07	0.61
	5	0.08	0.11	1.69	0.06	0.05	33.21	0.04	0.00	0.04	0.01	62.03	97.34	4.09	2.17	99.51	1.73	3	8.08	0.92	0.27	0.63
Fig. 5(32)	4	0.22	0.32	1.31	0.08	0.00	32.24	0.16	0.14	0.02	0.01	63.14	97.63	4.82	2.55	100.18	1.67	3	7.92	1.08	0.33	0.64
Fig. 5(33)	3	0.11	0.63	0.57	0.07	0.01	36.63	0.09	0.04	0.00	0.02	57.33	95.50	-0.09	-0.05	95.45	2.04	3	9.02	-0.02	-0.04	0.60
	4	0.28	0.68	0.68	0.06	0.00	35.63	0.19	0.03	0.00	0.01	57.46	95.02	0.25	0.13	95.15	2.01	3	8.94	0.06	-0.01	0.60
Fig. 5(34)	1	0.13	0.32	0.92	0.06	0.00	38.09	0.10	0.10	0.03	0.01	57.59	97.35	-0.93	-0.49	96.86	2.10	3	9.22	-0.22	-0.10	
	5	0.11	0.29	1.04	0.07	0.00	36.47	0.09	0.11	0.04	0.02	58.79	97.02	0.66	0.35	97.37	1.98	3	8.85	0.15	0.02	0.60
Fig. 5(35)	1	0.30	0.26	1.91	0.13	0.00	39.29	0.79	0.08	0.00	0.01	51.39	94.17	-6.17	-3.27	90.90	2.56	3	10.54	-1.54	-0.56	
	9	0.16	0.03	0.46	0.06	0.00	35.49	0.43	0.08	0.02	0.00	57.22	93.96	0.77	0.41	94.36	1.95	3	8.82	0.18	0.05	0.61
	10	0.08	0.92	0.94	0.04	0.00	38.17	0.16	0.07	0.00	0.00	57.38	97.75	-1.54	-0.82	96.93	2.17	3	9.37	-0.37	-0.17	
Fig. 5(36)	1	15.91	1.82	1.02	0.36	0.00	24.64	8.14	0.05	0.16	1.21	39.03	92.34	-36.22	-19.18	73.15	5.10	3	19.13	-10.13	-3.10	
	3	0.14	0.05	1.92	0.06	0.00	37.27	0.07	0.06	0.04	0.04	59.11	98.74	0.07	0.04	98.78	2.04	3	8.98	0.02	-0.04	0.60
Fig. 5(37)	1	0.00	0.34	4.02	0.00	0.00	47.28	0.00	0.02	0.00	0.01	54.04	105.71	-9.36	-4.96	100.75	2.92	3	11.46	-2.46	-0.92	
	2	0.00	0.33	2.84	0.06	0.00	42.13	0.00	0.04	0.00	0.00	56.88	102.30	-4.41	-2.34	99.96	2.43	3	10.09	-1.09	-0.43	
	6	0.13	0.38	2.21	0.07	0.00	32.77	0.13	0.11	0.03	0.02	61.30	97.15	3.40	1.80	98.95	1.80	3	8.23	0.77	0.20	0.63
Fig. 5(38)	1	0.15	0.42	1.20	0.10	0.00	32.39	0.14	0.07	0.02	0.01	63.14	97.66	4.80	2.54	100.20	1.68	3	7.93	1.07	0.32	0.64
	5	0.36	0.45	1.12	0.19	0.00	24.90	0.27	0.10	0.05	0.01	67.16	94.62	10.83	5.73	100.35	1.27	3	6.72	2.28	0.73	0.70
Fig. 5(39)	1	0.57	0.11	0.87	0.20	0.00	26.40	1.07	0.17	0.04	0.03	68.47	97.93	9.49	5.03	102.95	1.34	3	6.99	2.01	0.66	0.69
	5	0.74	0.25	0.85	0.29	0.00	20.77	1.39	0.29	0.07	0.08	72.09	96.82	13.54	7.17	103.99	1.10	3	6.24	2.76	0.90	0.73

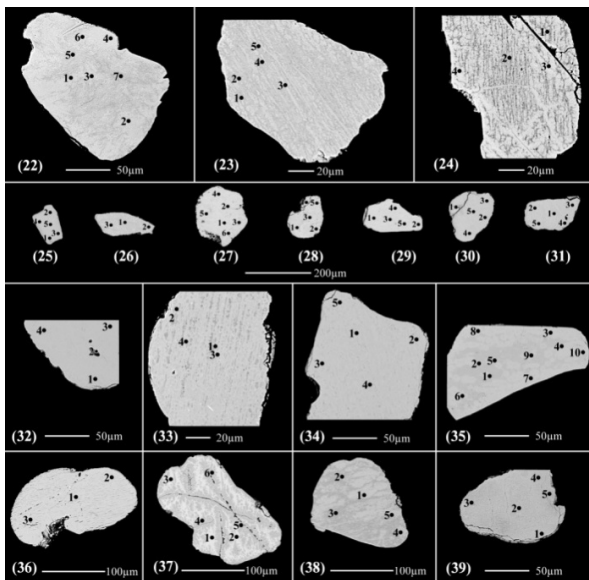


Fig. 5. BSE images of the black altered ilmenite grains (22)-(39), separated as magnetic at 0.25 A.

In Figure 5, grains (28)-(32) consist of well-defined psr phases. Spots 1-3 in grain (33) are leached ilmenite where the TiO₂ content ranges between 56.95 and 57.33 wt % and the

Fe₂O₃ content ranges between 37.82 and 36.63 wt %. Spot 4 is psr with some molecular water. the analyzed TiO₂ (57.46 wt %) and Fe₂O₃ (35.63 wt %) are relatively higher than those recorded. The correction of these values by multiplying by [100/(100- 4.85)], gives 60.45 wt % for TiO₂ and 37.48 wt % for Fe₂O₃. Spots 1-4 in grain (34) are leached ilmenite while spot 5 is psr with Ti/Ti+Fe ratio of 0.6. In grain (35), spots 1-10, except spot 9, are leached ilmenite. They have TiO₂ content ranging between 51.39 and 57.38 wt % and Fe₂O₃ content ranging between 39.3 and 38.17 wt %. Spot 9 is psr, with a Ti/Ti+Fe ratio of 0.61. According to the OT values, most of these spots contain molecular water between 8.66 and 2.25 wt %.

In grain (36) (Figure 5, Table IV), spot 1 is a composite between an inclusion of SiO₂ and leached ilmenite or psr. Spots 2 and 4 are leached ilmenite. It is obvious that some little amount of Fe⁺⁺ is still present in the structure. Spot 3 is psr with a Ti/Ti+Fe ratio equal to 0.6. Spots 1 and 2 of grain (37) are not ilmenite, but leached ilmenite. Most iron content seems to be Fe⁺⁺. Some individual TiO₂ phases, most probably rutile, are present with the ilmenite as a solid solution. Spots 3-6 are psr. They have TiO₂ content ranging between 59.7 and 61.3 wt %, Fe₂O₃ content ranging between 32.77 and 36.66 wt %, and Ti/Ti+Fe ratio ranging between 0.6 and 0.63. Spots 1-5 of grain (38) are psr. The TiO₂ content ranges between 63.14 and 67.16

wt %, the Fe_2O_3 content between 24.9 and 32.39 wt %, and the Ti/Ti+Fe ratio between 0.64 and 0.70. Some of the TiO_2 content was mixed with the original ilmenite. The amount of TiO_2 which is not included in the psr formula and/or the content of included structural water in psr may affect the darkness of the color of the analyzed spots. Spots 1-5 in grain (39) are psr. The TiO_2 content ranges between 68.47 and 72.09 wt %, the Fe_2O_3 content between 20.77 and 26.40 wt %, and the Ti/Ti+Fe ratio between 0.69 and 0.73. This grain was originally exsolved intergrowth of titanhematite-ferrilmenite, where most of the hematite content was leached. Some individual TiO_2 and/or Fe_2O_3 phases are still mixed with the formed psr. Hence, the calculated NT is much more than 100 wt %. The psr-lpsr of these investigated grains have the chemical formula range of $\text{Fe}_{2.07-1.1}\text{Ti}_3\text{O}_{8.83-6.24}(\text{OH})_{0.17-2.76}$ (Table IV). Only 2 spot analyses have Fe content ranging between 2.01 and 2.03 due to the appreciable contents of Mn and/or Mg which have oxidation state of 2^+ .

C. The Separated Magnetic Fraction at 0.35 A

1) The Investigated Dark Brown Grains

The investigated dark brown grains are the grains (1)-(12) (Figure 6, Table V). Except of spots 1 of (2), 2 of (11) and 1 and 2 of (12), most of the other analyzed spots are psr. In these grains, the TiO_2 content ranges between 58.69 and 73.92 wt %, the Fe_2O_3 content ranges between 14.42 and 33.38 wt %, and the Ti/Ti+Fe ratio ranges between 0.62 and 0.80. All the analyzed spots of grain (1) are psr. The spots in grain (2) are psr and lpsr, except spot 1 which consists of remnants of leached ilmenite. In grain (3), the original grain seems to be ferrilmenite-titanhematite exsolved intergrowth where most of the contained hematite was leached out during the alteration to psr. When comparing spots 1 and 7 regarding their MnO% and $\text{Fe}_2\text{O}_3\%$ content, it is obvious that the content of MnO is directly correlated with the content of Fe_2O_3 . Grain (4) includes different phases of lpsr. In spots 4 and 5, both SiO_2 and Al_2O_3 contents are relatively higher due to the decreasing content of Fe_2O_3 while the MnO content is relatively lower. At a definite decreasing limit of Fe_2O_3 content inside the lpsr phase, the MnO content starts to diminish while the opposite occurs in relation to SiO_2 and Al_2O_3 . Also, the reason of the darkness of the BSE of spots 4 and 5 is most probably the increasing content of the included structural water. Spot 1 in grain (5) is psr. The remaining spots are composed of various phases of lpsr. Spots 4, 5, and 7 reflect that the increased SiO_2 and Al_2O_3 content may be correlated with the decreased Fe_2O_3 content. In grain (6), the psr of spots 1-3 is different than that of spots 4 and 5. In spots 4 and 5, either the calculated amount of structural water is incorrect or not all the recorded TiO_2 content is contained within the lpsr phase, and some of the analyzed TiO_2 is present as individual phases which were originally mixed with the original ilmenite or were separated individually outside the lpsr phase during the late alteration stages. The grains (7)-(9) are psr. The lpsr of spots 4-5 in grain (9) is different than that of spots 1-3. In grain (10), the NT of the analyzed spots is much more than 100%. So, either the calculated structural water is incorrect or there are mixed phases rather than the psr phase alone. Spots 1-5 have TiO_2 contents ranging between 70.09 and 78.04%, Fe_2O_3 content

between 12.64 and 22.68%, and Ti/Ti+Fe ratio between 0.73 and 0.82. In spots 6 and 7, the contained lpsr phase is most probably broken out into definite individual phases of TiO_2 and Fe_2O_3 . The enrichment of SiO_2 content seems to be correlated directly with the enriched individual TiO_2 phase. Also, in these two last spots, the content of MnO is diminished due to the decreased Fe_2O_3 content (Table V).

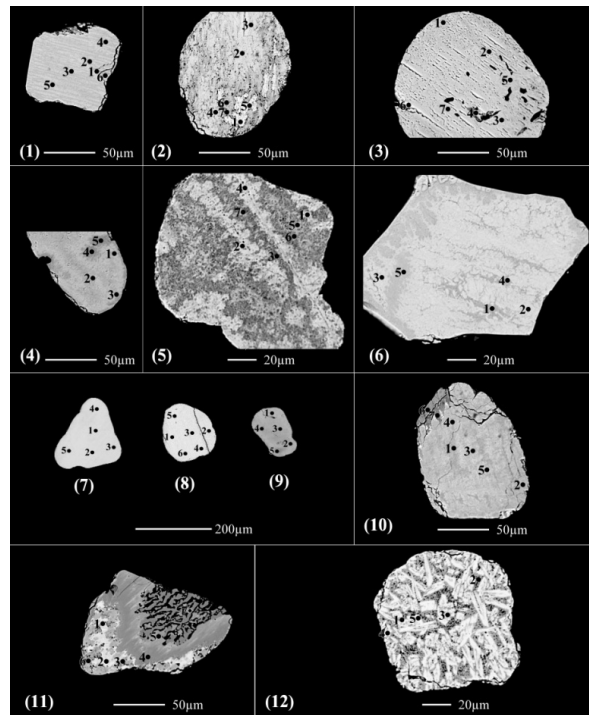


Fig. 6. BSE images of the brown altered ilmenite grains (1)-(12), separated as magnetic at 0.35 A.

Spot 1 of grain (11) was originally titanhematite altered to goethite. Spot 2 is leached ilmenite. Spots 3-6 are various phases of psr and lpsr. The darkness of some analyzed spots in the BSE image is due to the presence of structural and/or molecular water. Spot 7 is mixed individual phases of TiO_2 and Fe_2O_3 after psr. When comparing spots 1 and 7 regarding their contents of MnO% and $\text{Fe}_2\text{O}_3\%$, it is obvious that they are directly correlated. Spots 1 and 2 of grain (12) are leached ilmenite while spot 3 is psr. Spots 4 and 5 are lpsr of different phase than that of spot 3. In spots 4 and 5, either the calculated structural water is incorrect or not all the recorded TiO_2 content is included in the lpsr phase. There is an enrichment of an individual TiO_2 phase. The psr-lpsr of the investigated brown altered ilmenite grains have the chemical formula range of $\text{Fe}_{1.65-0.66}\text{Ti}_3\text{O}_{7.88-4.96}(\text{OH})_{1.12-4.04}$ (Table V). In spots 6, 7 of grain (10), spot 7 of grain (11), and spots 4 and 5 of grain (12), the content of cationic iron in the calculated psr-lpsr chemical formula ranges between 0.28 and 0.44. The investigation of the BSE images, especially of grains (10) and (11) ensures the change of mineral phases into an individual TiO_2 mineral phase, most probably rutile. Then, these cationic Fe values are discarded as minimum values for the existence of psr-lpsr phases.

TABLE V. MICROPROBE CHEMICAL ANALYSES AND THE CORRESPONDING MOLECULAR FORMULAE OF THE ANALYZED SPOTS OF THE BROWN ALTERED ILMENITE GRAINS (1)-(22) OF FIGURE 6, SEPARATED AS MAGNETIC AT 0.35 A

Grain	Spot	SiO ₂	MgO	MnO	CaO	ZnO	Fe ₂ O ₃	Al ₂ O ₃	Cr ₂ O ₃	Na ₂ O	K ₂ O	TiO ₂	OT	OH%	H ₂ O%	NT	Fe ₂	Ti ₃	Ox	OHy	Lost Fe	Ti/(Ti+Fe)
Fig. 6(1)	1	0.38	0.09	0.49	0.25	0.07	26.00	0.40	0.12	0.03	0.02	63.89	91.74	9.49	5.03	96.77	1.34	3	6.98	2.02	0.66	0.69
	6	0.24	0.09	0.48	0.16	0.06	24.79	0.42	0.09	0.02	0.01	65.89	92.24	11.24	5.95	98.19	1.23	3	6.64	2.36	0.77	0.71
Fig. 6(2)	1	1.54	0.19	1.96	0.08	0.11	37.46	0.69	0.08	0.00	0.05	54.91	97.07	-4.48	-2.38	94.69	2.38	3	10.09	-1.09	-0.38	
	7	0.21	0.09	0.30	0.16	0.00	23.54	0.25	0.11	0.03	0.01	69.47	94.18	13.44	7.12	101.30	1.09	3	6.23	2.77	0.91	0.73
Fig. 6(3)	1	0.50	0.19	1.58	0.24	0.00	26.93	0.59	0.06	0.03	0.00	62.17	92.29	7.28	3.85	96.14	1.50	3	7.42	1.58	0.50	0.67
	7	0.61	0.19	0.98	0.17	0.02	23.95	1.48	0.11	0.03	0.03	65.92	93.47	9.89	5.24	98.71	1.32	3	6.91	2.09	0.68	0.69
Fig. 6(4)	4	0.45	0.12	0.90	0.26	0.03	23.01	0.35	0.11	0.02	0.00	67.33	92.56	12.44	6.59	99.15	1.16	3	6.42	2.58	0.84	0.72
	5	1.29	0.17	0.50	0.29	0.03	18.73	0.81	0.06	0.01	0.01	69.42	91.31	14.83	7.86	99.16	1.00	3	6.01	2.99	1.00	0.75
Fig. 6(5)	1	0.39	0.20	1.75	0.09	0.04	33.38	0.11	0.04	0.01	0.00	58.69	94.70	2.09	1.11	95.81	1.87	3	8.52	0.48	0.13	0.62
	5	1.58	0.31	0.89	0.31	0.09	22.70	0.61	0.15	0.00	0.04	64.38	91.05	9.87	5.23	96.28	1.31	3	6.92	2.08	0.69	0.70
	7	1.20	0.31	0.47	0.34	0.02	18.24	0.53	0.13	0.00	0.04	67.72	89.00	14.98	7.93	96.94	1.00	3	5.98	3.02	1.00	0.75
Fig. 6(6)	1	0.33	0.12	0.62	0.21	0.11	26.91	0.25	0.10	0.00	0.03	65.42	94.10	9.47	5.02	99.12	1.34	3	6.98	2.02	0.66	0.69
	2	0.45	0.13	0.46	0.28	0.20	23.90	0.33	0.16	0.02	0.02	67.89	93.84	12.06	6.39	100.22	1.18	3	6.49	2.51	0.82	0.72
	5	0.33	0.10	0.50	0.33	0.22	20.45	0.31	0.11	0.01	0.01	71.65	94.02	15.66	8.29	102.32	0.96	3	5.84	3.16	1.04	0.76
Fig. 6(7)	5	0.65	0.22	0.83	0.25	0.07	24.80	0.65	0.13	0.04	0.05	67.28	94.96	10.47	5.54	100.51	1.28	3	6.79	2.21	0.72	0.70
Fig. 6(8)	6	0.19	0.10	1.53	0.32	0.09	26.33	0.27	0.07	0.00	0.01	65.79	94.69	9.64	5.10	99.79	1.35	3	6.94	2.06	0.65	0.69
Fig. 6(9)	1	0.58	0.19	0.63	0.30	0.05	20.32	0.79	0.31	0.02	0.02	69.50	92.71	14.23	7.54	100.24	1.05	3	6.11	2.89	0.95	0.74
	3	0.59	0.16	0.66	0.29	0.03	20.17	0.77	0.34	0.00	0.02	70.12	93.16	14.51	7.68	100.84	1.03	3	6.06	2.94	0.97	0.74
	5	0.75	0.17	0.36	0.40	0.07	14.42	1.05	0.46	0.00	0.00	73.92	91.59	19.10	10.12	101.70	0.77	3	5.29	3.71	1.23	0.80
Fig. 6(10)	1	0.47	0.15	0.44	0.24	0.15	22.68	0.58	0.51	0.01	0.01	70.09	95.33	13.03	6.90	102.23	1.12	3	6.32	2.68	0.88	0.73
	5	0.80	0.15	0.20	0.37	0.07	12.64	0.71	1.02	0.04	0.02	78.04	94.04	21.11	11.18	105.22	0.66	3	4.96	4.04	1.34	0.82
	6	1.61	0.23	0.07	0.61	0.08	4.34	0.75	0.92	0.03	0.04	80.75	89.44	26.64	14.11	103.55	0.38	3	4.16	4.84	1.62	0.89
	7	1.45	0.13	0.08	0.60	0.00	4.03	0.78	0.97	0.03	0.04	84.35	92.45	27.46	14.55	107.00	0.34	3	4.03	4.97	1.66	0.90
Fig. 6(11)	1	0.17	0.05	0.41	0.14	0.09	86.88	0.24	0.04	0.03	0.01	1.82	89.88	-91.87	-48.65	41.23	145.63	3	438.52	-429.52	-143.63	
	2	0.18	0.10	3.14	0.05	0.07	37.70	0.00	0.06	0.00	0.01	55.99	97.29	-2.22	-1.17	96.12	2.24	3	9.54	-0.54	-0.24	
	3	0.31	0.02	2.36	0.11	0.09	30.89	0.08	0.04	0.01	0.02	63.21	97.12	5.46	2.89	100.02	1.64	3	7.78	1.22	0.36	0.65
	6	0.30	0.13	0.24	0.11	0.02	16.94	0.09	0.09	0.02	0.01	76.69	94.63	19.88	10.53	105.16	0.72	3	5.13	3.87	1.28	0.81
	7	3.40	0.86	0.02	0.10	0.00	3.70	1.03	0.06	0.03	0.05	87.53	96.79	25.96	13.75	110.54	0.41	3	4.31	4.69	1.59	0.88
Fig. 6(12)	1	0.38	0.19	1.31	0.25	0.07	39.74	0.48	0.18	0.00	0.01	53.87	96.49	-4.74	-2.51	93.98	2.42	3	10.17	-1.17	-0.42	
	4	2.88	0.02	0.26	0.23	0.03	7.58	0.07	0.11	0.00	0.01	84.42	95.62	24.86	13.17	108.78	0.44	3	4.43	4.57	1.56	0.87
	5	0.45	0.03	0.18	0.13	0.00	6.72	0.07	0.13	0.00	0.01	86.84	94.58	28.54	15.12	109.69	0.28	3	3.84	5.16	1.72	0.92

2) The Investigated Black Grains

The investigated grains from (13) to (25) (Figure 7, Table VI), are composed of leached ilmenite, psr, and lpsr. Spots from 1 to 4 of grain (24) and spot 4 of grain (25) are leached ilmenite. The spots of psr and lpsr have TiO₂ content ranging between 56.76 and 70.20 wt %, Fe₂O₃ content ranging between 22.02 and 36.13 wt %, and Ti/Ti+Fe ratio ranging between 0.6 and 0.74. Both grains (13) and (14) are composed of psr. In grain (15), spots 1 to 3 are psr of definite chemical composition while spots 4, 5 are another psr phase. The regions of these two last spots are relatively darker due to the increasing content of included structural water. The spots of grain (16) are psr. The grains (17), (18), and (19) are psr. In grain (20), the spots from 1 to 7 are psr. Spot 5 is inside a relatively large fissure where the rate of alteration is relatively higher. Hence, due to the relatively higher leaching rate of Fe⁺⁺⁺ from the psr, the structure is broken and most Fe₂O₃ content is hydrolyzed (or hydroxylated) by the water captured by silica and/or alumina or by water containing both. That is the reason for the enrichment of SiO₂ and Al₂O₃ in spot 5. Spots 8 and 9 of grain (20) are lpsr of different formulas than those of spots 6 and 7. Spots 8 and 9 spots have more structural water, hence they have relatively darker BSE image regions. This grain seems that was originally ferriilmenite associated with several titanhematite exsolved bodies which were leached out causing several empty pits. The

analyzed spots of grain (21) are psr. Spot 1 of grain (22) is a definite altered silicate mineral. The remaining analyzed spots of grains (22), (23) are mainly psr. Grains (21), (22), (23) were originally titanhematite-ferriilmenite exsolved intergrowths.

Most titanhematite components have been leached out leaving partially empty small pits and voids or longitudinal cracks in grain (21). These empty spaces are favorable locations for saturation with molecular water. That is the reason for the relative values of OT and NT. Grain (23) contains the lowest psr chemical composition (spot 1). The original ilmenite of this grain was mixed with the pyrophanite component, hence the content of MnO ranges between 2.33 and 6.85 wt %. The investigation of grains (22) and (23) may indicate that the presence of the original titanhematite component accelerates the rate of alteration for the associated ferriilmenite component. In grain (24), spots 1-4 are leached ilmenite while spots 5-8 are psr. In spots 5-8, the TiO₂ content ranges between 57.59 and 58.2 wt %, the Fe₂O₃ content ranges between 35.62 and 37.22 wt % and the Ti/Ti+Fe ratio range between 0.60 and 0.61. Also, the total oxide sum indicates that most of the analyzed spots contain molecular water. Grain (25) is composed of leached ilmenite (spot 4), and psr (spots 3, 5, and 6). Spots 5 and 6 have a Ti/Ti+Fe ratio ranging between 0.68 and 0.70. Spots 1 and 2 are definite silicate mineral composites with individual TiO₂ phase. Comparing the BSE images of spots 1

and 2 indicates that the increased SiO₂ content causes the relative dark color of the spot area. The psr-lpsr of these investigated magnetic black altered grains have the chemical formula range of Fe_{2.02-1.06}Ti₃O_{9-6.15}(OH)_{0-2.85} (Table VI). Only one spot analysis gave Fe content of 2.02 due to the appreciable content of Mn.

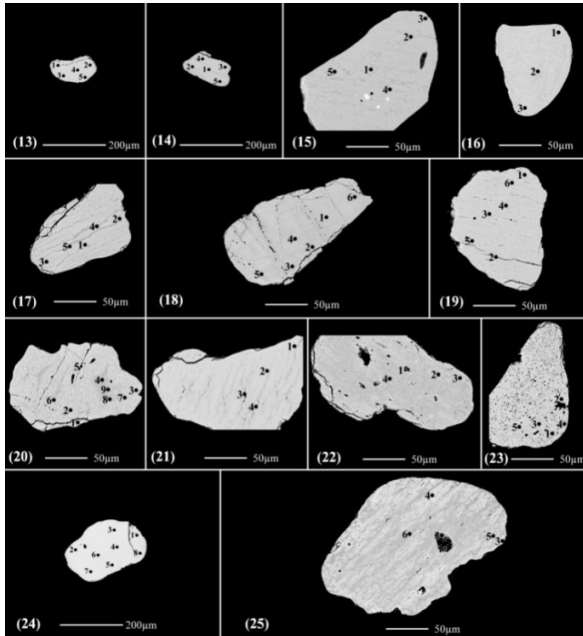


Fig. 7. BSE images of the black altered ilmenite grains (13)-(25), separated as magnetic at 0.35 A.

The psr-lpsr chemical formulas of all the investigated altered ilmenite grains of Figures 2-7 and Tables I-VI are: Fe_{2.07-0.54}Ti₃O_{9-4.68}(OH)_{0-4.32}. The Ti/(Ti+Fe) ratio for these formulas ranges between 0.59 and 0.85. The given values of the Ti/(Ti+Fe) ratios for psr in the literature are different: 0.5-0.7 [32], 7-0.7 [31], 0.6-0.7 [33], 0.6 [34], and 0.6-0.79 or 0.80 [35]. The given lower limit of [32] for psr is not precise, it is overlapped with the phases of ilmenite and leached ilmenite.

D. The Detected Leached Ilmenite Analyzed Spots

Forty two spots were analyzed and detected to be leached ilmenite within all the studied altered ilmenite grains. The analysis of these spots did not give the psr/lpsr chemical formulas. In these 42 spots, taking into consideration that the ilmenite chemical formula is Fe₃Ti₃O₉, the contents of TiO₂, FeO, and Fe₂O₃ range between 51.39-59.19, 39.84-0.02, and 3-37.02, respectively. The cationic Fe²⁺ ranges between 0 and 2.46, while the cationic Fe³⁺ ranges between 0.17 and 1.94. The Ti/(Ti+Fe) ratio ranges between 0.51 and 0.6, almost the same as that reported in [33]. The Fe/Ti ratio ranges between 0.91 and 0.67 (Table VII), which is different than that given by [36] which is 1.02 and decreases to about 0.84 for pseudoilmenite and to 0.64 for pseudorutile. Although the new calculated NT ranges between 90.24 and 101.27 wt %, most of its values are much less than 100 wt %. This reflects the role of molecular water in the process of ilmenite alteration into leached ilmenite. Note that in Table VII, the other cations are composed mainly

of Mg and Mn whereas the oxide percentages of other cations (SiO₂, Al₂O₃, Cr₂O₃, Na₂O₃ and K₂O) are minor.

According to [31], leached ilmenite stable up to the composition of Fe_{2.35-2.3}Ti₃O₉ with TiO₂ wt % ranges between 56 and 58 wt %. In the present study (Table VII), where the leached ilmenite formulas have the composition Fe_{2.72-2.02}Ti₃O₉ with the minimum value of iron equal to 2.02 (grain (24) of Figure 7, spot 3). There are two methods for calculating the lost Fe²⁺ cations of ilmenite Fe₃Ti₃O₉ and leached ilmenite:

In the first method (M1), the sum of total Fe²⁺ and Fe³⁺ iron in addition to all other cations except Ti (mainly Mg and Mn) must be subtracted from 3. The number of iron cations in the given ilmenite formula structure (Fe₃Ti₃O₉) is:

$$\text{Lost iron} = 3 - [\text{total iron} + \text{all other cations except Ti}] \quad (13)$$

The second one (M2), is an established rule by the present author: It has been explained [37, 38] that the FeTiO₃ structure is derived from α -Fe₂O₃ by replacing every layer of Fe atoms in the (0001) planes by a layer of Ti atoms, thus producing alternating layers of Fe and Ti atoms between slightly distorted, hexagonally close-packed O layers. By the losing of one Fe²⁺ cation, two Fe²⁺ cations are oxidized into two Fe³⁺ cations to meet the deficiency of the two lost positive charges from the ilmenite-leached ilmenite structure. The number of the lost Fe²⁺ cations corresponds to half the number of the formed Fe³⁺ inside the leached ilmenite structure. It also corresponds to the deficiency of the calculated oxygen anion number normalized to 3 Ti in the leached ilmenite structure. This number must be equal to 9 when there is no losing of Fe²⁺ iron outside the given ilmenite formula structure (Fe₃Ti₃O₉):

$$\begin{aligned} \text{Number of lost Fe}^{2+} \text{ cations} &= \text{half the number of formed Fe}^{3+} \text{ cations} \\ &= \text{deficiency of the calculated normalized oxygen to 3 Ti.} \end{aligned} \quad (14)$$

In fact, there is a difference of the calculated lost iron by using the two most postulated methods. The value of lost iron calculated with the first method is relatively higher than that calculated with the second, due to one or more of the following:

- Some of the existing Fe³⁺ cations are related to an individual Fe₂O₃ component present in association with ilmenite, not to the ilmenite mineral structure, in the analyzed spot.
- Some individual TiO₂ components are present with ilmenite. Then, in calculating the normalized cations on the basis of 3 Ti, all the calculated cation values are affected. The percentage of the individual TiO₂ component is mixed and contained within the total analyzed TiO₂ of the spot, hence the calculated Ti-factor (3/the calculated Ti cations), will be relatively lower, causing the lowering of the calculated Fe cations when normalized to 3 Ti. A relatively higher value of the calculated lost iron is obtained.
- If some of the ferrous iron is substituted with other definite cations, the lost Fe²⁺ iron may be not offsetted with the oxidation of two Fe²⁺ into two Fe³⁺ cations. For example, if Fe²⁺ is replaced with Al³⁺ or Si⁴⁺ then:

$$2 \text{Al}^{3+} = 3 \text{Fe}^{2+}, \text{ or } \text{Si}^{4+} = 2 \text{Fe}^{2+} \quad (15)$$

In the first equation, one Fe^{2+} is lost without a corresponding formation of Fe^{3+} . In this case, the number of lost iron equals to half the number of the present Al^{3+} in the analyzed spot. In the second equation, one Fe^{2+} is lost without a corresponding formation of Fe^{3+} . In this case, the number of lost iron equals to the number of the present Si^{4+} in the analyzed spot. Then, an electrical neutralization in the leached ilmenite crystal structure can occur due to the substitution of Fe^{2+} cations with other cations of relatively higher oxidation number (3^+ or 4^+) without the formation of the corresponding Fe^{3+} cations. This explanation may be the reason for the following correct relation in the analyzed leached ilmenite spots of the present study (Table VII):

$$\text{Calculated lost iron by the first method} - \text{the calculated lost iron by the second method} = \text{Si}^{4+} + 0.5 \text{Al}^{3+} \quad (16)$$

However, the majority of the analyzed leached ilmenite spots contain negligible amounts of Si and Al and maybe CaO,

Na_2O , and K_2O . If these oxides are treated as impurities, the most major analyzed oxide (TiO_2) in the spot will be affected by the correction of the analyzed oxide values. Hence, the calculated Ti-factor (3/the calculated Ti cations), will be relatively lower, leading to the lowering of the calculated Fe cations normalized to 3 Ti. Hence, the calculated lost iron value using the first method of calculation, will be relatively bigger. Finally, it was remarked that the microprobe chemical analyses of some detected ilmenite spots have TiO_2 content similar to those classified as leached ilmenite (TiO_2 ranges between 56 and 59 wt %). This analysis does not response to the adopted chemical formula of leached ilmenite. The sum of all the analyzed oxides in each of these spots is very close to, or slightly lower than, 100 wt %. In these spots, the occurrence of solid solutions or exsolved intergrowth of TiO_2 with ilmenite are postulated. It maybe also, exsolved intergrowths of titanhematite where a selective leaching of the Fe_2O_3 component occurs, resulting in an enrichment of the TiO_2 -bearing component in the analyzed spots.

TABLE VI. MICROPROBE CHEMICAL ANALYSES AND THE CORRESPONDING MOLECULAR FORMULAE OF THE ANALYZED SPOTS OF THE BLACK ALTERED ILMENITE GRAINS (13)-(25) OF FIGURE 7, SEPARATED AS MAGNETIC AT 0.35 A

Grain	Spot	SiO ₂	MgO	MnO	CaO	ZnO	Fe ₂ O ₃	Al ₂ O ₃	Cr ₂ O ₃	Na ₂ O	K ₂ O	TiO ₂	OT	OH %	H ₂ O %	NT	Fe ₂	Ti ₃	Ox	OHy	Lost Fe	Ti/(Ti+Fe)
Fig. 7(13)	1	0.92	0.67	0.75	0.13	0.02	30.59	0.38	0.06	0.06	0.01	60.76	94.36	3.96	2.10	96.45	1.73	3	8.12	0.88	0.27	0.63
	5	0.23	0.41	0.67	0.13	0.00	31.05	0.16	0.03	0.00	0.02	62.44	95.14	5.67	3.00	98.14	1.61	3	7.74	1.26	0.39	0.65
Fig. 7(14)	1	0.98	0.22	2.34	0.10	0.08	28.12	0.61	0.04	0.04	0.03	62.03	94.59	5.40	2.86	97.45	1.64	3	7.80	1.20	0.36	0.65
	5	0.68	0.26	1.72	0.25	0.13	23.76	0.52	0.08	0.04	0.03	67.36	94.84	10.80	5.72	100.56	1.28	3	6.73	2.27	0.72	0.70
Fig. 7(15)	3	0.28	0.13	0.74	0.19	0.00	28.78	0.41	0.06	0.00	0.04	64.99	95.60	7.95	4.21	99.81	1.44	3	7.28	1.72	0.56	0.68
	4	0.36	0.17	0.62	0.26	0.03	25.39	0.48	0.07	0.04	0.00	67.75	95.17	10.94	5.80	100.96	1.25	3	6.70	2.30	0.75	0.71
	5	0.46	0.16	0.51	0.28	0.00	22.02	0.46	0.13	0.05	0.00	70.20	94.27	13.93	7.38	101.65	1.06	3	6.15	2.85	0.94	0.74
Fig. 7(16)	3	0.14	0.37	1.53	0.09	0.11	32.53	0.10	0.06	0.04	0.01	59.50	94.47	3.21	1.70	96.17	1.80	3	8.27	0.73	0.20	0.62
Fig. 7(17)	1	0.13	0.07	0.62	0.09	0.06	31.10	0.14	0.02	0.01	0.01	61.43	93.66	5.75	3.04	96.71	1.59	3	7.73	1.27	0.41	0.65
	5	0.55	0.10	0.59	0.22	0.00	24.36	0.37	0.13	0.03	0.03	65.87	92.26	11.08	5.87	98.13	1.24	3	6.68	2.32	0.76	0.71
Fig. 7(18)	1	0.20	0.15	2.00	0.12	0.09	29.05	0.08	0.03	0.00	0.01	62.36	94.06	6.65	3.52	97.58	1.55	3	7.54	1.46	0.45	0.66
	6	0.30	0.12	1.36	0.15	0.03	26.13	0.18	0.09	0.02	0.00	65.73	94.12	9.91	5.25	99.37	1.32	3	6.89	2.11	0.68	0.69
Fig. 7(19)	1	0.29	0.77	0.90	0.10	0.00	31.79	0.10	0.02	0.02	0.02	59.90	93.90	3.76	1.99	95.89	1.76	3	8.15	0.85	0.24	0.63
	2	0.07	0.88	2.03	0.05	0.07	32.12	0.00	0.00	0.04	0.01	60.39	95.65	3.40	1.80	97.45	1.81	3	8.23	0.77	0.19	0.62
	6	0.22	0.61	0.64	0.12	0.04	31.00	0.11	0.03	0.03	0.01	62.94	95.74	5.76	3.05	98.79	1.61	3	7.73	1.27	0.39	0.65
Fig. 7(20)	1	0.15	0.05	2.18	0.10	0.01	33.84	0.02	0.02	0.00	0.02	57.03	93.42	1.38	0.73	94.15	1.94	3	8.68	0.32	0.06	0.61
	5	1.34	0.28	1.66	0.21	0.01	27.52	0.50	0.04	0.02	0.04	59.27	90.89	4.74	2.51	93.40	1.67	3	7.95	1.05	0.33	0.64
	6	0.06	0.08	2.76	0.11	0.06	31.89	0.02	0.00	0.00	0.00	59.57	94.55	3.55	1.88	96.43	1.79	3	8.19	0.81	0.21	0.63
	7	0.19	0.07	2.97	0.12	0.07	29.96	0.02	0.05	0.03	0.00	60.28	93.75	4.84	2.57	96.32	1.70	3	7.91	1.09	0.30	0.64
	8	0.46	0.15	1.49	0.28	0.16	24.63	0.18	0.03	0.02	0.01	65.24	92.64	10.44	5.53	98.16	1.29	3	6.79	2.21	0.71	0.70
Fig. 7(21)	1	0.12	0.17	1.59	0.08	0.04	33.46	0.11	0.07	0.01	0.02	58.99	94.65	2.57	1.36	96.01	1.84	3	8.41	0.59	0.16	0.62
	4	0.24	0.22	1.44	0.13	0.09	30.97	0.54	0.05	0.04	0.01	59.47	93.18	3.87	2.05	95.23	1.75	3	8.13	0.87	0.25	0.63
Fig. 7(22)	1	23.49	1.87	1.15	0.65	0.08	14.84	17.36	0.04	0.05	0.26	25.80	85.58	-73.18	-38.75	46.83	9.29	3	33.67	-24.67	-7.29	
	2	2.05	0.36	2.82	0.11	0.03	23.26	0.84	0.01	0.01	0.05	53.15	82.68	3.38	1.79	84.47	1.78	3	8.24	0.76	0.22	0.63
	3	0.22	0.11	2.97	0.08	0.18	32.52	0.05	0.10	0.03	0.02	57.85	94.13	1.92	1.02	95.15	1.92	3	8.56	0.44	0.08	0.61
Fig. 7(23)	1	0.15	0.37	2.33	0.07	0.09	33.78	0.15	0.04	0.00	0.01	56.76	93.75	0.77	0.41	94.15	2.00	3	8.82	0.18	0.00	0.60
	5	0.08	0.29	2.66	0.04	0.05	31.70	0.01	0.04	0.02	0.00	59.72	94.60	3.61	1.91	96.51	1.79	3	8.18	0.82	0.21	0.63
Fig. 7(24)	1	1.49	0.23	0.82	0.07	0.00	36.68	0.74	0.04	0.02	0.03	55.43	95.56	-3.13	-1.66	93.90	2.24	3	9.75	-0.75	-0.24	
	4	0.07	0.15	0.83	0.06	0.00	37.53	0.05	0.07	0.03	0.00	57.32	96.11	-0.33	-0.18	95.93	2.05	3	9.08	-0.08	-0.05	
	5	0.11	0.14	0.94	0.06	0.16	35.62	0.06	0.06	0.00	0.01	57.59	94.76	0.90	0.48	95.24	1.96	3	8.79	0.21	0.04	0.61
	8	0.09	0.13	0.82	0.07	0.00	36.16	0.09	0.10	0.00	0.01	58.20	95.68	0.90	0.48	96.15	1.95	3	8.79	0.21	0.05	0.61
Fig. 7(25)	1	18.15	0.44	0.07	0.21	0.06	4.59	19.01	0.02	0.07	0.04	43.43	86.09	-33.70	-17.85	68.24	4.15	3	16.99	-7.99	-2.15	
	2	6.77	0.17	0.40	0.18	0.04	15.14	14.11	0.04	0.00	0.01	48.21	85.05	-14.42	-7.64	77.41	2.95	3	12.33	-3.33	-0.95	
	3	0.16	0.22	0.75	0.10	0.00	36.13	0.10	0.04	0.01	0.02	57.03	94.56	0.29	0.15	94.71	2.00	3	8.93	0.07	0.00	0.60
	4	0.07	0.89	0.65	0.06	0.10	36.16	0.05	0.03	0.02	0.01	57.06	95.09	-0.11	-0.06	95.03	2.06	3	9.03	-0.03	-0.06	
	5	0.28	0.30	0.11	0.16	0.02	28.33	0.18	0.03	0.00	0.01	62.80	92.21	8.00	4.24	96.45	1.43	3	7.27	1.73	0.57	0.68
	6	0.45	0.25	0.03	0.19	0.07	26.03	0.25	0.03	0.05	0.03	65.18	92.54	10.16	5.38	97.92	1.29	3	6.85	2.15	0.71	0.70

TABLE VII. MICROPROBE CHEMICAL ANALYSES AND THE CORRESPONDING MOLECULAR FORMULAE OF THE DETECTED ANALYZED SPOTS OF LEACHED ILMENITE FROM THE DIFFERENT MAGNETIC ALTERED ILMENITE GRAIN VARIETIES

Grain	Spot	SiO ₂	MgO	MnO	CaO	ZnO	FeO	Al ₂ O ₃	Cr ₂ O ₃	Na ₂ O	K ₂ O	TiO ₂	OT	NT	FeO %	Fe ₂ O ₃ %	Fe ferrous	Fe ferric	Other cations	Total Fe	Ti	O	Lost Fe (M1)	Lost Fe (M2)	Si	Al	Si+0.5Al	Ti/(Ti+Fe)	Fe/Ti
Fig. 3(16)	1	0.09	0.14	2.28	0.06	0.00	34.38	0.00	0.05	0.03	0.00	59.19	96.21	99.74	2.54	35.37	0.14	1.79	0.16	2.10	3	9	0.90	0.90	0.01	0.00	0.01	0.59	0.70
Fig. 3(18)	3	0.31	0.13	1.67	0.07	0.00	33.59	0.15	0.02	0.05	0.03	57.45	93.47	96.78	3.80	33.10	0.22	1.73	0.16	2.11	3	9	0.89	0.86	0.02	0.01	0.03	0.59	0.70
	4	0.15	0.08	1.80	0.03	0.00	34.85	0.05	0.02	0.00	0.02	57.88	94.87	98.14	5.40	32.72	0.31	1.70	0.13	2.14	3	9	0.86	0.85	0.01	0.00	0.01	0.58	0.71
	4	0.01	0.14	2.17	0.02	0.00	39.98	0.00	0.02	0.00	0.00	52.13	94.48	95.45	31.20	9.75	2.00	0.56	0.16	2.72	3	9	0.28	0.28	0.00	0.00	0.00	0.52	0.91
Fig. 3(20)	5	0.00	0.17	1.63	0.02	0.11	40.31	0.00	0.00	0.00	0.00	52.29	94.54	95.57	31.01	10.33	1.98	0.59	0.13	2.70	3	9	0.30	0.30	0.00	0.00	0.00	0.53	0.90
	6	0.00	0.19	1.79	0.02	0.07	39.56	0.00	0.00	0.00	0.00	52.76	94.39	95.65	28.20	12.62	1.78	0.72	0.14	2.64	3	9	0.36	0.36	0.00	0.00	0.00	0.53	0.88
Fig. 4(1)	1	0.18	0.60	0.53	0.06	0.10	35.94	0.10	0.06	0.00	0.01	57.78	95.36	98.36	8.86	30.09	0.51	1.56	0.13	2.20	3	9	0.80	0.78	0.01	0.01	0.02	0.58	0.73
	2	0.08	0.66	0.66	0.06	0.14	34.56	0.08	0.07	0.00	0.01	58.50	94.82	98.27	3.47	34.54	0.20	1.77	0.13	2.10	3	9	0.90	0.89	0.01	0.01	0.01	0.59	0.70
	3	0.07	0.66	0.55	0.06	0.05	34.64	0.05	0.11	0.01	0.00	58.52	94.72	98.21	3.25	34.88	0.19	1.79	0.12	2.10	3	9	0.90	0.89	0.00	0.00	0.01	0.59	0.70
	4	0.08	0.66	0.70	0.06	0.01	34.10	0.09	0.06	0.03	0.01	58.66	94.45	98.05	1.68	36.02	0.10	1.84	0.13	2.07	3	9	0.93	0.92	0.01	0.01	0.01	0.59	0.69
	5	0.22	0.75	0.66	0.08	0.00	33.38	0.13	0.10	0.00	0.01	59.03	94.37	98.07	0.07	37.01	0.00	1.88	0.15	2.04	3	9	0.96	0.94	0.01	0.01	0.02	0.60	0.68
Fig. 4(2)	2	0.09	0.45	1.02	0.10	0.14	33.84	0.06	0.07	0.00	0.00	58.06	93.83	97.35	2.13	35.23	0.12	1.82	0.13	2.08	3	9	0.92	0.91	0.01	0.00	0.01	0.59	0.69
	5	0.06	0.63	0.91	0.06	0.00	33.71	0.03	0.03	0.03	0.01	58.57	94.02	97.71	0.51	36.88	0.03	1.89	0.13	2.05	3	9	0.95	0.95	0.00	0.00	0.00	0.59	0.68
Fig. 5(33)	1	0.08	0.62	0.61	0.04	0.10	37.82	0.06	0.00	0.00	0.01	56.95	96.28	98.77	15.37	24.94	0.90	1.31	0.12	2.34	3	9	0.66	0.66	0.01	0.01	0.01	0.56	0.78
	2	0.40	0.66	0.73	0.07	0.14	35.44	0.30	0.02	0.00	0.00	57.21	94.98	97.70	10.89	27.28	0.63	1.43	0.18	2.24	3	9	0.76	0.72	0.03	0.03	0.04	0.57	0.75
	3	0.11	0.63	0.57	0.07	0.01	36.63	0.09	0.04	0.00	0.02	57.33	95.50	98.30	11.39	28.04	0.66	1.47	0.12	2.25	3	9	0.75	0.73	0.01	0.01	0.01	0.57	0.75
Fig. 5(34)	1	0.13	0.32	0.92	0.06	0.00	34.28	0.10	0.10	0.03	0.01	57.59	93.54	96.92	3.81	33.85	0.22	1.76	0.12	2.10	3	9	0.90	0.88	0.01	0.01	0.01	0.59	0.70
	2	0.06	0.30	0.77	0.05	0.00	34.94	0.04	0.10	0.01	0.00	57.60	93.87	97.23	4.72	33.58	0.27	1.75	0.09	2.12	3	9	0.88	0.87	0.00	0.00	0.01	0.59	0.71
	3	0.12	0.16	1.09	0.04	0.00	33.99	0.08	0.09	0.07	0.00	57.73	93.36	96.88	2.31	35.19	0.13	1.83	0.11	2.08	3	9	0.92	0.91	0.01	0.01	0.01	0.59	0.69
	4	0.13	0.33	1.20	0.05	0.00	33.57	0.08	0.10	0.04	0.00	58.03	93.51	97.09	1.32	35.83	0.08	1.85	0.13	2.06	3	9	0.94	0.93	0.01	0.01	0.01	0.59	0.69
Fig. 5(35)	1	0.30	0.26	1.91	0.13	0.00	35.36	0.79	0.08	0.00	0.01	51.39	90.23	91.51	23.79	12.85	1.54	0.75	0.27	2.56	3	9	0.44	0.38	0.02	0.07	0.06	0.54	0.85
	2	0.42	0.10	0.56	0.14	0.00	35.37	0.81	0.09	0.04	0.01	51.72	89.26	90.88	20.71	16.29	1.34	0.95	0.18	2.46	3	9	0.54	0.47	0.03	0.07	0.07	0.55	0.82
	3	0.33	0.13	0.77	0.10	0.00	32.62	0.71	0.09	0.05	0.02	52.90	87.71	90.24	9.90	25.23	0.62	1.43	0.17	2.23	3	9	0.77	0.72	0.02	0.06	0.06	0.57	0.74
	4	0.23	0.17	3.07	0.06	0.00	32.49	0.54	0.10	0.04	0.02	54.72	91.43	93.96	9.76	25.26	0.59	1.39	0.29	2.27	3	9	0.73	0.69	0.02	0.05	0.04	0.57	0.76
	5	0.15	0.57	1.71	0.07	0.00	34.21	0.36	0.08	0.01	0.02	55.63	92.81	95.42	10.75	26.06	0.64	1.41	0.22	2.27	3	9	0.73	0.70	0.01	0.03	0.03	0.57	0.76
	6	0.16	0.73	1.25	0.06	0.00	34.31	0.26	0.08	0.02	0.01	56.03	92.90	95.65	9.52	27.54	0.57	1.48	0.20	2.24	3	9	0.76	0.74	0.01	0.02	0.02	0.57	0.75
	7	0.09	1.28	0.67	0.06	0.00	34.08	0.22	0.07	0.02	0.00	56.37	92.86	95.70	8.52	28.39	0.50	1.51	0.21	2.23	3	9	0.77	0.76	0.01	0.02	0.02	0.57	0.74
	8	0.12	0.26	2.08	0.05	0.00	33.04	0.26	0.05	0.00	0.01	56.88	92.73	95.97	3.85	32.43	0.23	1.71	0.19	2.12	3	9	0.88	0.86	0.01	0.02	0.02	0.59	0.71
	10	0.08	0.92	0.94	0.04	0.00	34.35	0.16	0.07	0.00	0.00	57.38	93.93	97.04	6.33	31.13	0.37	1.63	0.18	2.17	3	9	0.83	0.81	0.01	0.01	0.01	0.58	0.72
Fig. 5(36)	2	0.09	0.02	1.66	0.02	0.00	34.53	0.01	0.06	0.02	0.00	58.75	95.14	98.75	2.02	36.12	0.11	1.85	0.11	2.07	3	9	0.93	0.92	0.01	0.00	0.01	0.59	0.69
	4	0.10	0.07	2.10	0.07	0.00	33.81	0.01	0.06	0.04	0.03	59.11	95.40	99.08	0.62	36.87	0.03	1.87	0.15	2.06	3	9	0.94	0.94	0.01	0.00	0.01	0.59	0.69
Fig. 5(37)	1	0.00	0.34	4.02	0.00	0.00	42.54	0.00	0.02	0.00	0.01	54.04	100.97	101.27	39.84	3.00	2.46	0.17	0.29	2.92	3	9	0.08	0.08	0.00	0.00	0.00	0.51	0.97
	2	0.00	0.33	2.84	0.06	0.00	37.91	0.00	0.04	0.00	0.00	56.88	98.08	100.21	18.66	21.40	1.09	1.13	0.21	2.43	3	9	0.57	0.56	0.00	0.00	0.00	0.55	0.81
Fig. 6(2)	1	1.54	0.19	1.96	0.08	0.11	33.71	0.69	0.08	0.00	0.05	54.91	93.32	95.06	17.98	17.47	1.09	0.96	0.33	2.38	3	9	0.62	0.48	0.11	0.06	0.14	0.56	0.79
Fig. 6(11)	2	0.18	0.10	3.14	0.05	0.07	33.92	0.00	0.06	0.00	0.01	55.99	93.51	96.28	9.02	27.67	0.54	1.48	0.22	2.24	3	9	0.76	0.74	0.01	0.00	0.01	0.57	0.75
Fig. 6(12)	1	0.38	0.19	1.31	0.25	0.07	35.76	0.48	0.18	0.00	0.01	53.87	92.51	94.39	18.87	18.77	1.17	1.05	0.21	2.42	3	9	0.58	0.52	0.03	0.04	0.05	0.55	0.81
	2	0.21	0.24	1.18	0.18	0.00	32.86	0.43	0.21	0.02	0.02	57.69	93.01	96.45	1.92	34.37	0.11	1.79	0.17	2.07	3	9	0.93	0.89	0.01	0.03	0.03	0.59	0.69
	1	1.49	0.23	0.82	0.07	0.00	33.01	0.74	0.04	0.02	0.03	55.43	91.88	94.17	12.45	22.85	0.75	1.24	0.26	2.24	3	9	0.76	0.62	0.11	0.06	0.14	0.57	0.75
Fig. 7(24)	2	0.06	0.14	0.83	0.07	0.13	34.03	0.05	0.05	0.00	0.00	56.96	92.31	95.77	2.82	34.67	0.17	1.83	0.09	2.08	3	9	0.92	0.91	0.00	0.00	0.01	0.59	0.69
	3	0.08</																											

8(3)), while the sample after heating gave the composition of pseudobrookite, rutile, quartz and, only one line for hematite (Figure 8(4)). It is obvious that minor contents of amorphous hydrated silica were contained with psr. After heating, the water molecules were lost and the SiO_2 was recrystallized into minor quartz. Also, a considerable amount of TiO_2 content was separated from the relatively unstable psr structure and formed the relatively more stable rutile structure. The remaining TiO_2 and Fe_2O_3 of the unstable psr were modified into pseudobrookite. Some Fe_2O_3 , either from the psr structure or contained as an amorphous phase was recrystallized as minor hematite. The sample of the non-heated black colored variety gave the composition of psr and hematite (Figure 8(5)), while the sample after heating gave the composition of pseudobrookite, rutile and, only one line for hematite (Figure 8(6)). The same interpretation of the brown variety is correct except that the content of the associated amorphous Fe_2O_3 is relatively more here.

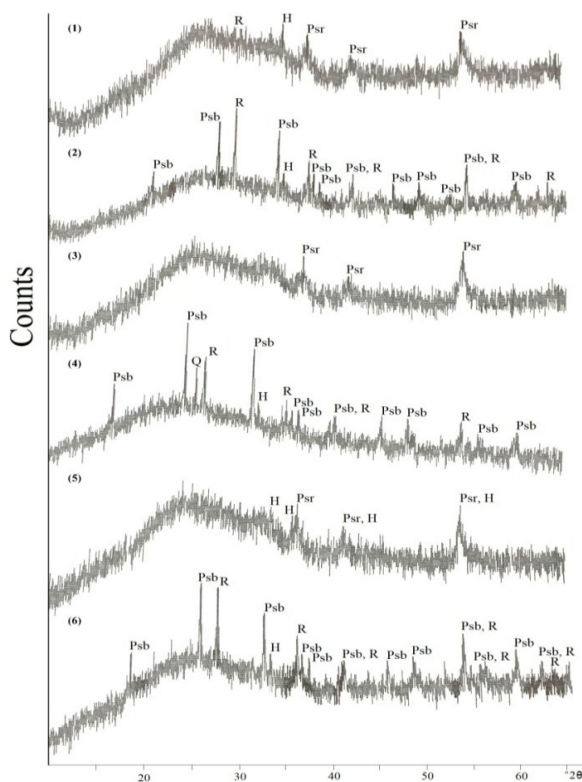


Fig. 8. XRDs of the different altered ilmenite grains: The magnetic altered ilmenite of 0.25 A (1) before and (2) after heating. The magnetic brown altered ilmenite of 0.35 A (3) before and (4) after heating. The magnetic black altered ilmenite of 0.35 A (5) before and (6) after heating.

The detected mineral patterns are in accordance to the ASTM card numbers 4-0551 for rutile, 19-182 for pseudorutile, 9-182 for pseudobrookite, 13-534 for hematite, and 4-0477 for anatase. It is worth mentioning that in the last two magnetic fractions, at 0.25 and 0.35 A, after heating, most of the stained and/or coated materials changed into translucent-transparent yellow and red rutile.

VI. CONCLUSIONS

In the detected leached ilmenite spots, the cationic Fe^{2+} ranges between 0 and 2.46, while the cationic Fe^{3+} ranges between 0.17 and 1.94. The $\text{Ti}/(\text{Ti}+\text{Fe})$ ratio ranges between 0.51 and 0.6, and the Fe/Ti ratio ranges between 0.91 and 0.67. The leached ilmenite formulas have the composition range of $\text{Fe}_{2.72-2.02}\text{Ti}_3\text{O}_9$ with a minimum value of iron equal to 2.02. In leached ilmenite, the number of lost Fe^{2+} cations is equal to half the number of formed Fe^{3+} cations which is equal to the deficiency of the calculated normalized oxygen to 3 Ti.

In the analyzed spots of psr-lpsr, the contents of TiO_2 and Fe_2O_3 range between 56.76-78.09 wt % and 37.98-12.16 wt %, respectively. The $\text{Ti}/(\text{Ti}+\text{Fe})$ ratio ranges between 0.60-0.82. The psr-lpsr chemical formula is: $\text{Fe}_{2.07-0.54}\text{Ti}_3\text{O}_{9-4.68}(\text{OH})_{0-4.32}$.

The cationic Fe content ranges between 0.28 and 0.44 values are discarded as minimum for the existence of psr-lpsr phases. It is concluded that the lower cationic iron content of still present lpsr phases is 0.5 with a corresponding molecular formula of $\text{Fe}_{0.5}\text{Ti}_3\text{O}_{4.5}(\text{OH})_{4.5}$. The concluded molecular formula of the present study is different than others proposed in the literature. The lower chemical composition formula limit of psr is $\text{Fe}_2\text{Ti}_3\text{O}_9$ [21], $\text{Fe}_{1.5}\text{Ti}_3\text{O}_{7.5}(\text{OH})_{1.5}$ [33], while authors in [31] reported that the average composition of lpsr has the formula $\text{FeTi}_3\text{O}_6(\text{OH})_3$, and the lower stability limit lies around 0.6 mol% Fe or slightly higher, as related to 3 mole% Ti. It is noticed that the process of leucoexanation is selective and relatively faster in the exsolved component (like the titanhematite component), or the replacement component (like the sphene component) within the altered ilmenite grain. The remaining fresh ilmenite component within the same grain has a relatively slow rate of alteration and seems to be altered later.

The comparison between the original OT and NT for the various spot chemical analyses of the detected grains reflects that the calculated structural water content values of some of the analyzed spots are incorrect, whereas not all the analyzed TiO_2 wt % is contained within the calculated psr/lpsr formulas. There are other individual phases of TiO_2 mixed with the lpsr phase. It was concluded that in the region of 68-70 TiO_2 wt %, the mechanism of ilmenite alteration is maybe changed. Some spots of altered silicate minerals can be falsely considered as psr and lpsr according to their chemical compositions. Also, it is obvious that the dependence on the powdered XRD analysis may be not enough to give correct results during the investigation of some analyzed spots related to psr and lpsr. The single crystal XRD may be a more efficient technique in such situations. Some of the associated contained inclusions may be responsible for the acquired magnetic characteristics of some detected grains.

In many published studies, both the recorded SiO_2 and Al_2O_3 contents are considered as impurities and must be subtracted from the total oxide sum followed by the recalculation and correction of the other analyzed oxides. However, the most abundant analyzed oxide, TiO_2 , of the spot will be highly affected by the recalculation and correction. It increases with a relatively bigger percentage than the other analyzed oxides, especially Fe_2O_3 , the second most abundant oxide of the spot analysis. If SiO_2 and/or Al_2O_3 are originally

associated with only TiO_2 or with only Fe_2O_3 then, some misleading results will be obtained. The content of structural water contained in the lpsr phase increases, as the associated SiO_2 and/or Al_2O_3 contents increase. In fact, most of the spots having an appreciable content of molecular water contain relatively higher contents of SiO_2 and Al_2O_3 . This may indicate the ability of these two oxides of bearing molecular water, or OH^- anions, or both. SiO_2 and Al_2O_3 may be associated with the molecular water itself. It is noticed that the content of MnO is directly correlated with the content of Fe_2O_3 .

The XRD power patterns of the detected different magnetic altered ilmenite grains ensure the presence of several mineral phases in the altered grains. They give the composition of either only pseudorutile or psr associated with hematite and maybe also rutile. After heating, all the obtained patterns contain pseudobrookite in addition to rutile and hematite and maybe quartz. In these heated altered varieties, it is obvious that the hematite is minor. Also, the hexagonal psr structure is unstable in comparison with the tetragonal rutile, a considerable TiO_2 content escaped from the broken psr structure and was diffused inside the rutile structure. The remaining TiO_2 and most of the Fe_2O_3 contents of the broken psr were modified into the orthorhombic pseudobrookite structure. Also, a minor content of amorphous hydrated silica contained with psr was detected after heating. The water molecules were lost and the SiO_2 was recrystallized into minor quartz.

ACKNOWLEDGEMENT

The author wishes to express his deepest gratitude to Dr. H.J. Massonne, Dr. Thomas Theye and the microprobe unit of the Institute of Mineralogy and Crystal Chemistry, Stuttgart University, Germany, for providing the microprobe analysis facilities.

REFERENCES

- [1] C. Palmer, "Arizonite, ferric metatitanate," *American Journal of Science*, vol. 28, pp. 353–356, Oct. 1909, <https://doi.org/10.2475/ajs.s4-28.166.353>.
- [2] J. L. Overholt, G. Vaux, and J. L. Rodda, "The nature of 'arizonite,'" *American Mineralogist*, vol. 35, no. 1–2, pp. 117–119, Feb. 1950.
- [3] L. E. Lynd, H. Sigurdson, C. H. North, and W. W. Anderson, "Characteristics of titaniferous concentrates," *Mining Engineering*, vol. 6, pp. 817–824, 1954.
- [4] V. T. Allen, "Is leucoxene always finely crystalline rutile?; discussion," *Economic Geology*, vol. 51, no. 8, pp. 830–833, Dec. 1956, <https://doi.org/10.2113/gsecongeo.51.8.830>.
- [5] S. A. Tyler and R. W. Marsden, "The nature of leucoxene," *Journal of Sedimentary Research*, vol. 8, no. 2, pp. 55–58, Aug. 1938, <https://doi.org/10.1306/D4268FEA-2B26-11D7-8648000102C1865D>.
- [6] S. W. Bailey, R. J. Weege, E. N. Cameron, and H. R. Spedden, "The alteration of ilmenite in beach sands," *Economic Geology*, vol. 51, no. 3, pp. 263–279, May 1956, <https://doi.org/10.2113/gsecongeo.51.3.263>.
- [7] S. W. Bailey and E. N. Cameron, "Is leucoxene always finely crystalline rutile?; reply," *Economic Geology*, vol. 52, no. 6, pp. 716–720, Sep. 1957, <https://doi.org/10.2113/gsecongeo.52.6.716>.
- [8] M. D. Karkhanavala, A. C. Momin, and S. G. Rege, "An x-ray study of leucoxene from Quilon, India," *Economic Geology*, vol. 54, no. 5, pp. 913–918, Aug. 1959, <https://doi.org/10.2113/gsecongeo.54.5.913>.
- [9] B. H. Flinter, "Malayan ilmenite vs. arizonite," *Economic Geology*, vol. 55, no. 5, pp. 1068–1070, Aug. 1960, <https://doi.org/10.2113/gsecongeo.55.5.1068>.
- [10] B. H. Flinter, "The alteration of Malayan ilmenite grains and the question of 'arizonite,'" *Economic Geology*, vol. 54, no. 4, pp. 720–729, Jun. 1959, <https://doi.org/10.2113/gsecongeo.54.4.720>.
- [11] L. E. Lynd, "Alteration of ilmenite," *Economic Geology*, vol. 55, no. 5, pp. 1064–1068, Aug. 1960, <https://doi.org/10.2113/gsecongeo.55.5.1064>.
- [12] A. K. Temple, "Alteration of ilmenite," *Economic Geology*, vol. 61, no. 4, pp. 695–714, Jun. 1966, <https://doi.org/10.2113/gsecongeo.61.4.695>.
- [13] N. P. Subrahmanyam, N. K. Rao, D. Narasimhan, G. V. U. Rao, N. K. Jaggi, and K. R. P. M. Rao, "Alteration of beach sand ilmenite from Manavalakurichi: Tamil Nadu, India," *Journal of Geological Society of India*, vol. 23, no. 4, pp. 168–174, 1982.
- [14] A. D. Bykov, "Proarizonite as a secondary mineral due to supergene alteration of ilmenite," *Doklady Akademii nauk SSSR*, vol. 156, pp. 567–570, 1964.
- [15] S. R. Austin, "Ilmenite, magnetite, and feldspar alteration under reducing conditions," *Economic Geology*, vol. 55, no. 8, pp. 1758–1759, Dec. 1960, <https://doi.org/10.2113/gsecongeo.55.8.1758>.
- [16] J. W. Gruner, "The decomposition of ilmenite; discussion," *Economic Geology*, vol. 54, no. 7, pp. 1315–1316, Nov. 1959, <https://doi.org/10.2113/gsecongeo.54.7.1315>.
- [17] D. Carroll, "Ilmenite alteration under reducing conditions in unconsolidated sediments," *Economic Geology*, vol. 55, no. 3, pp. 618–619, May 1960, <https://doi.org/10.2113/gsecongeo.55.3.618>.
- [18] J. A. Hartman, "The titanium mineralogy of certain bauxites and their parent materials," *Economic Geology*, vol. 54, no. 8, pp. 1380–1405, Dec. 1959, <https://doi.org/10.2113/gsecongeo.54.8.1380>.
- [19] F. Dimanche and P. Bartholome, "The alteration of ilmenite in sediments," *Minerals Science Engineering*, vol. 8, no. 3, pp. 187–200, 1976.
- [20] M. T. Frost, I. E. Grey, I. R. Harrowfield, and C. Li, "Alteration profiles and impurity element distributions in magnetic fractions of weathered ilmenite," *American Mineralogist*, vol. 71, no. 1–2, pp. 167–175, Feb. 1986.
- [21] I. E. Grey and A. F. Reid, "The structure of pseudorutile and its role in the natural alteration of ilmenite," *American Mineralogist*, vol. 60, no. 9–10, pp. 898–906, Oct. 1975.
- [22] R. R. Anand and R. J. Gilkes, "Some alumina and silica in weathered ilmenite grains is present in clay minerals a response to Frost et al. (1983)," *Mineralogical Magazine*, vol. 49, no. 350, pp. 141–145, Mar. 1985, <https://doi.org/10.1180/minmag.1985.049.350.25>.
- [23] E. F. Lener, "Mineral Chemistry of Heavy Minerals in the Old Hickory Deposit, Sussex and Dinwiddie Counties, Virginia," M.S. thesis, Virginia Tech, Blacksburg, VA, USA, 1997.
- [24] C. C. Gonçalves and P. F. A. Braga, "Heavy Mineral Sands in Brazil: Deposits, Characteristics, and Extraction Potential of Selected Areas," *Minerals*, vol. 9, no. 3, Mar. 2019, Art. no. 176, <https://doi.org/10.3390/min9030176>.
- [25] A.-A. M. Abdel-Karim, S. M. Zaid, M. I. Moustafa, and M. G. Barakat, "Mineralogy, chemistry and radioactivity of the heavy minerals in the black sands, along the northern coast of Egypt," *Journal of African Earth Sciences*, vol. 123, pp. 10–20, Nov. 2016, <https://doi.org/10.1016/j.jafrearsci.2016.07.005>.
- [26] M. I. Moustafa, "Some Mineralogical Characteristics of the Egyptian Black Sand Beach Ilmenite Part I: Homogeneous Ilmenite and Titanhematite-Ferriilmenite Grains," *Engineering, Technology & Applied Science Research*, vol. 12, no. 6, pp. 9614–9631, Dec. 2022, <https://doi.org/10.48084/etasr.5296>.
- [27] M. I. Moustafa, "Some Mineralogical Characteristics of the Egyptian Black Sand Beach Ilmenite Part II: Rutile-Ilmenite and the Various Titanhematite Grains," *Engineering, Technology & Applied Science Research*, vol. 12, no. 6, pp. 9640–9653, Dec. 2022, <https://doi.org/10.48084/etasr.5297>.
- [28] T. Chernet and L. Pakkanen, "Estimation of ferric iron, crystal water and calculation of chemical formulae for altered ilmenite from electron microprobe analyses, based on stoichiometric criteria," *Geological Survey of Finland*, vol. 36, pp. 23–28, 2003.

- [29] M. I. Moustafa, "Mineralogical Characteristics of the Separated Magnetic Rutile of the Egyptian Black Sands," *Resource Geology*, vol. 60, no. 3, pp. 300–312, 2010, <https://doi.org/10.1111/j.1751-3928.2010.00130.x>.
- [30] M. I. Moustafa, "Mineralogy and beneficiation of some economic minerals in the Egyptian black sands," Ph.D. dissertation, Mansoura University, Mansoura, Egypt, 1999.
- [31] A. Mucke and J. N. Bhadra Chaudhuri, "The continuous alteration of ilmenite through pseudorutile to leucoxene," *Ore Geology Reviews*, vol. 6, no. 1, pp. 25–44, Feb. 1991, [https://doi.org/10.1016/0169-1368\(91\)90030-B](https://doi.org/10.1016/0169-1368(91)90030-B).
- [32] G. Pe-Piper, D. J. W. Piper, and L. Dolansky, "Alteration of ilmenite in the Cretaceous sandstones of Nova Scotia, southeastern Canada," *Clays and Clay Minerals*, vol. 53, no. 5, pp. 490–510, Oct. 2005, <https://doi.org/10.1346/CCMN.2005.0530506>.
- [33] M. T. Frost, I. E. Grey, I. R. Harrowfield, and K. Mason, "The dependence of alumina and silica contents on the extent of alteration of weathered ilmenites from Western Australia," *Mineralogical Magazine*, vol. 47, no. 343, pp. 201–208, Jun. 1983, <https://doi.org/10.1180/minmag.1983.047.343.10>.
- [34] S. Tetsopgang, J. Koyanagi, M. Enami, and K. Kihara, "Hydroxylian pseudorutile in an adamellite from the Nkambe area, Cameroon," *Mineralogical Magazine*, vol. 67, no. 3, pp. 509–516, Jun. 2003, <https://doi.org/10.1180/0026461036730113>.
- [35] I. E. Grey and C. Li, "Hydroxylian pseudorutile derived from picroilmenite in the Murray Basin, southeastern Australia," *Mineralogical Magazine*, vol. 67, no. 4, pp. 733–747, Aug. 2003, <https://doi.org/10.1180/0026461036740130>.
- [36] S. S. Ahmed, M. Y. Miah, C. Qumruzzaman, M. N. Zaman, A. B. Alam, and P. K. Biswas, "Alteration and Exsolution Characteristics of Ilmenites of Moheskhali Island, Chittagong, Bangladesh," *Bangladesh Journal of Scientific and Industrial Research*, vol. 45, no. 1, pp. 17–26, 2010, <https://doi.org/10.3329/bjsir.v45i1.5173>.
- [37] C. Klein and S. Hurlbut, *Manual of Mineralogy*, 21st Edition. New York, NY, USA: John Wiley & Sons, 1993.
- [38] R. A. Fellows, A. R. Lennie, A. W. Munz, D. J. Vaughan, and G. Thornton, "Structures of FeTiO₃ (0001) surfaces observed by scanning tunneling microscopy," *American Mineralogist*, vol. 84, no. 9, pp. 1384–1391, Sep. 1999, <https://doi.org/10.2138/am-1999-0916>.
- [39] M. I. Moustafa, M. A. Tashkandi, and A. M. El-Sherif, "Detecting Mineral Resources and Suggesting a Physical Concentration Flowsheet for Economic Minerals at the Northern Border Region of Saudi Arabia," *Engineering, Technology & Applied Science Research*, vol. 12, no. 3, pp. 8617–8627, Jun. 2022, <https://doi.org/10.48084/etasr.4894>.